INTERNATIONAL ATOMIC ENERGY AGENCY
UNITED NATIONS EDUCATIONAL, SCIENTIFIC AND CULTURAL ORGANIZATION

INTERNATIONAL CENTRE FOR THEORETICAL PHYSICS
34100 TRIESTE (ITALY) - P.O.B. 586 - MIRAMARE - STRADA COSTIERA 11 - TELEPHONE: 2240-1
CABLE: CENTRATOM - TELEX 460392 - I

H4.SMR 346/ 34

SCHOOL ON
NON-ACCELERATOR PHYSICS
25 April - 6 May 1988

ATTEMPTS TO DETECT ISOTOPES RESULTING FROM RARE NUCLEAR AND COSMOLOGICAL PROCESSES ARCHIVED IN GEOLOGICAL SAMPLES

by

C. Tuniz
Universite di Trieste
Italy

ATTEMPTS TO DETECT ISOTOPES RESULTING FROM RARE NUCLEAR AND COSMOLOGICAL PROCESSES ARCHIVED IN GEOLOGICAL SAMPLES

(ULTRA - HIGH SENSITIVITY MASS SPECTROMETRY)

Claudio Tuniz

Dipartimento di Fisica
Universita' di Trieste Italy

Outline:

New ultrasensitive analytical techniques

- Accelerator Mass Spectrometry (AMS)
- Resonance Ionization Spectrometry (RIS)

Rare processes

- Doble Beta Decay
- Proton decay
- Solar neutrino detectors

Rare particles

- Fractionally charged particles
- Heavy particles bound in nuclei

ACCELERATOR MASS SPECTROMETRY (AMS)

MOLECULAR BACKGROUND:
STRIPPING @HV TERMINAL

ISOBARIC BACKGROUND:
NEGATIVE IONS

ISOTOPIC BACKGROUND:
MAGNETIC & ELECTROSTATIC ANALYSIS

RESIDUAL BACKGROUND:
NUCLEAR ION DETECTOR

SENSITIVITY:

10^{-16}

NIM B29(1987)133

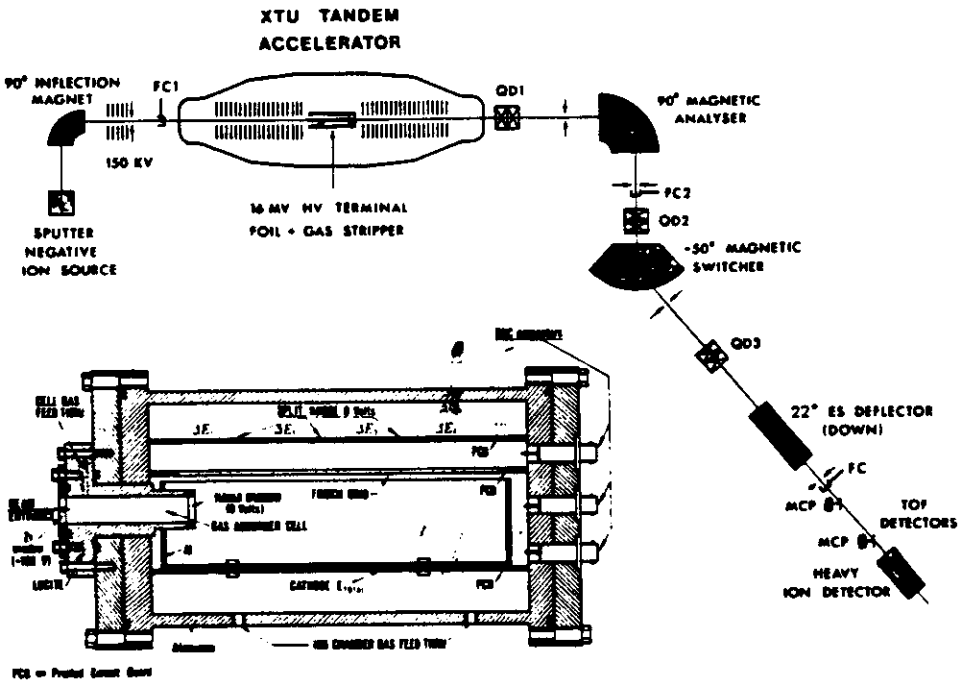

Fig. 1. Schematic diagram of the XTU tandem accelerator mass spectrometry system. The ionization chamber is shown in the lower left of the figure.

injector has a double focussing 90° magnet with mass resolution 1 : 100. The XTU tandem presently works at a maximum terminal voltage of about 15 MV. The beam transport system is designed for high magnetic rigidity (analysing magnet with mass energy product 500 MeV amu). A high-resolution 22° electrostatic deflector is located on the 50° beam line dedicated to AMS.

The following detectors for final identification of rare isotopes have been tested: Bragg chamber, multi-anode ionization chamber with absorber cell, time-of-flight system based on low-pressure multi-wire proportional counters and micro-channel plates.

During AMS measurements, the abundant isotope is transmitted only as far as the image position of the 90° analyzing magnet and is measured by integrating the current in a Faraday cup (FC2). The inflection magnet, the analyzing magnet and the high-energy quadrupole (QD1) are then scaled to transport the rare isotope. The latter is transmitted to the final detection system after further magnetic and electrostatic analysis. The focussing and deflection elements are optimized beforehand for maximum transmission of the rare isotope by injecting and transporting the abundant beam at the appropriate voltage.

Isotope ratios are measured by switching the magnetic elements mentioned above to select alternately the abundant and the rare isotope.

3. The electrostatic deflector

Reduction of isotopic background and other unwanted beams during AMS measurements is obtained by combining magnetic and electric analysis. A high-resolution electrostatic deflector has been added to our AMS system for this purpose.

The main characteristics of the deflector are: radius of curvature 5 m, length 2 m, deflection angle 22°, gap between the electrodes 2.5 cm. The two aluminum electrodes (designed and built at Ohio State University and University of Rochester) are supported by macor bars and precisely positioned inside a stainless steel tank. A cryogenic pump with a pumping speed of 1500 l/s keeps the vacuum inside the tank at about 10^{-8} Torr. With these vacuum conditions, a maximum electric field of 54 kV/cm (corresponding to $E/Q = 13.5$ MeV) was applied to the electrodes.

The beam is deflected downward rather than horizontally to separate energy analysis from position fluctuations of the beam after magnetic analysis. In fact, during AMS measurements, with GVM control and slits wide open, variations in terminal voltage produce a momentum spread of the beam in the horizontal plane. Typical terminal voltage variability with GVM control is ±5 kV at 8 MV.

Careful beam optics calculations were carried out to choose the correct position of the electrostatic deflector

between the last lens (QD3) and the detection system. Energy resolution of this analyzer is $\Delta E/E = 2 \times 10^{-3}$. Beam dimensions measured at the detector position are 3 mm in the vertical dimension and 7 mm in the horizontal dimension.

Two versatile devices for insertion of Faraday cups, collimators and absorbers have been installed upstream and downstream from the deflector.

In the following we show that electrostatic analysis completely rejects isotopic background during ^{10}Be and ^{36}Cl measurements. We are also exploring the possibility of using this system to separate isobars via energy or charge dispersion methods.

4. ^{10}Be measurements

Early ^{10}Be measurements were performed by using a telescope of silicon surface-barrier detectors with solid absorbers to eliminate ^{10}B [2]. In the last runs, an isobutane-filled ionization chamber of the Rochester type [4] was installed after the electrostatic analyzer for final identification (see insert of fig. 1). This chamber was designed and built in a collaboration with the Nuclear Physics Laboratory, Rutgers University, New Jersey (USA). The entrance window has a diameter of 1.8 cm. A segmented anode collects energy loss information in four regions of the detector. Each anode plate, 6.5 cm wide and 40 cm long, is maintained at ground potential. The total energy signal is derived from the ions collected at the cathode. The cathode is 19.4 cm long, and is capacitively coupled to the grid to collect the total charge of the ions in the beam. The cathode is biased to -700 V, the grid to -420 V. The cathode–grid spacing is 3.7 cm, the anode–grid spacing is 1.2 cm.

Gas flow through the detector prevents the build up of oxygen and other contaminants. The pressure used during ^{10}Be measurements was 70 Torr, sufficient to stop ^{10}Be at the third anode.

A removable gas cell stops the isobaric interference in front of the detector. The Havar entrance and exit window of the cell are bonded to brass support rings with conducting epoxy and work as electrodes. This cell is used as an ionization chamber for ^{10}B to check accelerator tuning and to monitor transmission stability during ^{10}Be measurements.

Fig. 2a shows a particle spectrum (second anode vs cathode signal) obtained in 3 min from a standard sample (^{10}Be/^{9}Be $= 1.21 \times 10^{-9}$). Typical ^{10}Be counting rates with this sample were 6 cps with a BeO^- current of 60 nA. Measurement were performed at a terminal voltage of 8 MV with charge state 3+.

Background measured with a BeO reagent blank was 3×10^{-3} cps ^{10}Be with a BeO^- current of 80 nA, corresponding to an isotopic ratio ^{10}Be/^{9}Be of 7×10^{-13}. Fig. 2b shows a background spectrum obtained in about 20 min. This background is due to ^{10}B reactions in the cell or to a contamination of our blank. Reduction of hydrogen in the absorber cell and lowering of terminal voltage should improve ^{10}B-induced background. Tests are in progress with a new blank kindly provided by the Pennsylvania group.

An attempt to measure ^{10}Be in ice samples from Monte Rosa (Italy) failed because of the low output of the 834 sputter source (typical BeO^- current was less than 80 nA). This problem could be solved by using our sputter source model GIC 860. Preliminary tests with this source gave a BeO^- current of about 1.5 μA from our sample of reagent BeO.

5. ^{36}Cl measurements

The ionization chamber described in the previous paragraph was used to identify ^{36}Cl in a standard

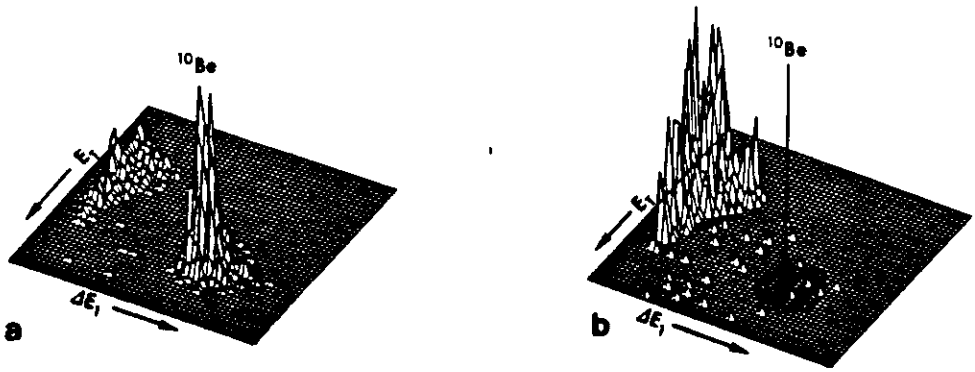

Fig. 2. Particle spectrum (ΔE vs total energy E) a) from a standard beryllium sample (^{10}Be/^{9}Be $= 1.21 \times 10^{-9}$); b) from BeO reagent blank. In both cases with electrostatic analysis.

sample and in two iron meteorites. In this case, the gas cell was replaced by a 1.5 μm thick mylar window and the isobutane pressure was kept at about 50 Torr to stop ^{36}Cl at the third anode.

^{36}Cl measurements were performed using charge state 7 at 7.75 MV. Interfering beams transmitted through the magnets are ^{35}Cl, ^{37}Cl and ^{36}S. ^{35}Cl is injected directly as $H^{35}Cl^-$ while ^{37}Cl can be injected when discharges inside the source drop the extraction voltage. ^{35,37}Cl beams can assume the same magnetic rigidity as mass 36 after charge-exchange in the accelerator tubes. Fig. 3a shows the presence of this background in a particle spectrum obtained with a Bragg chamber from a standard sample ($^{36}Cl/Cl = 2 \times 10^{-10}$) before the installation of the electrostatic deflector [3,5].

This isotopic interference which is transmitted with the same magnetic rigidity as the rare isotope is now completely removed by electrostatic analysis. As the physical separation between the ^{36}Cl and the other chlorine beams after electrostatic deflection is about 2 cm, a 1 cm wide collimator placed in front of the detector is sufficient to reject ^{35}Cl and ^{37}Cl. Fig. 3b shows the particle spectrum obtained under these conditions with the same sample as fig. 3a. This scatter plot represents signals from the second and third anode of the ionization chamber. The best isobaric separation is given by residual energy.

The present limitation in measuring ^{36}Cl with our system is due to sulphur which forms negative ions almost as readily as chlorine. The usual approach to reducing this background is chemical purification of the samples and the use of low-sulphur material to make sample holders for the ion source.

We adopted highly purified tantalum cones and tried ^{36}Cl measurements on samples prepared following various chemical procedures.

Typical $^{35}Cl^-$ output from our standard samples was in the range 5–10 μA. Stable beams are attenuated by a chopper located after the ion source in order to avoid beam loading of the tandem. The beam fraction selected during this experiment was 10%.

The counting rates for a purified standard sample ($^{36}Cl/Cl = 2.15 \times 10^{-10}$) were 143 cps of ^{36}S and 95 cps of ^{36}Cl with 6 μA of $^{35}Cl^-$. A blank sample consisting of reagent grade AgCl gave a $^{35}Cl^-$ current of 1 μA and counting rates of 400 cps for ^{36}S and 10^{-3} cps for ^{36}Cl, corresponding to $^{36}Cl/Cl = 10^{-13}$, due entirely to the low-energy tail of ^{36}S.

A ^{36}Cl spectrum from a sample of the iron meteorite Treysa, sample weight 0.7227 g, carrier Cl 1.0 mg activity 22 dpm/kg [6], is shown in fig. 4. Counting rates were 9 cps ^{36}Cl and 800 cps ^{36}S with a $^{35}Cl^-$ current of 1.7 μA.

The iron meteorite Carbo, sample weight 1.06 g carrier Cl 1.0 mg, activity 5.8–7.6 dpm/kg [7], gave counting rates of about 11 cps for ^{36}Cl and 1400 cps for ^{36}S, with a $^{35}Cl^-$ current of 2.6 μA.

The aim of the reported measurements was to test the performance of our detection system after the installation of the electrostatic deflector and the sulphur contamination of the meteorite samples.

In the future, we are planning to use total stripping and electrostatic analysis to reject sulphur background. At energies of about 200 MeV, a carbon foil of 1 $\mu g/cm^2$ produces fully stripped chlorine ions with 18% probability. After electric deflection, the separation between ^{36}Cl and ^{36}S is 4 cm. Beam focussing is not disturbed by the stripper. Low transmission caused by selection of charge 17 can be compensated by using the high intensity source. With a $^{37}Cl^-$ current of 100 μA, a sample with $^{36}Cl/Cl$ ratio of 10^{-14} would give about 40 counts per hour. Measurements to check this possibility are in progress.

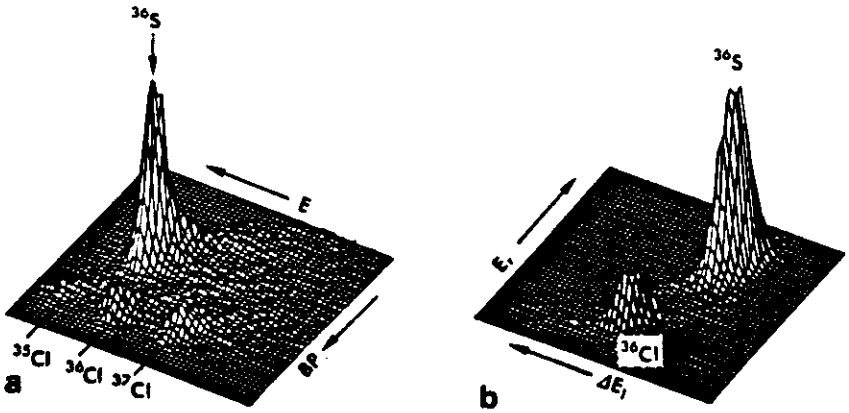

Fig. 3. Particle spectra from a standard chlorine sample ($^{36}Cl/Cl = 2 \times 10^{-10}$), a) with Bragg chamber (Bragg peak vs total energy and without electrostatic analysis, b) with multi-anode ionization chamber (ΔE vs residual energy) and electrostatic analysis.

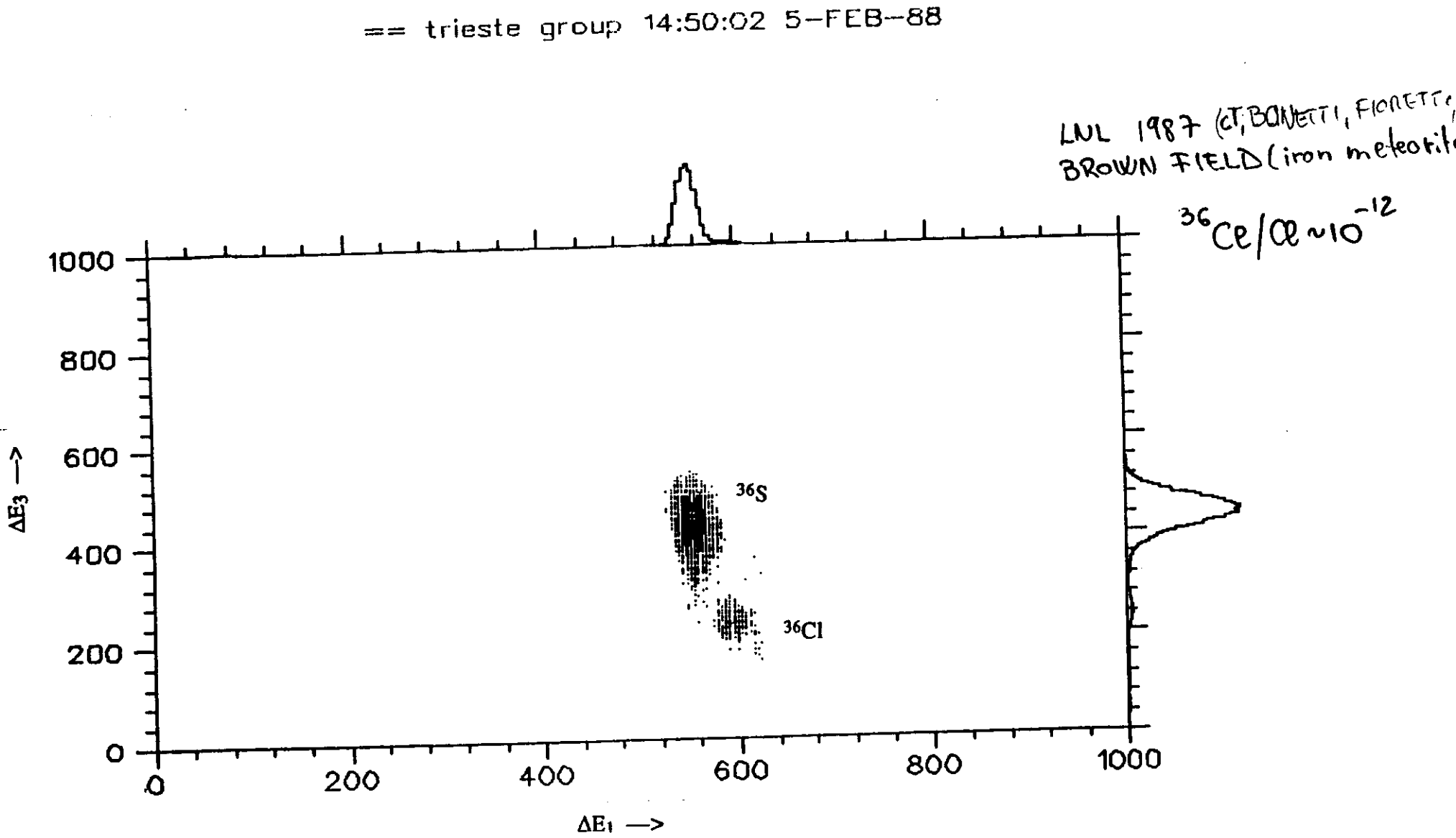
== trieste group 14:50:02 5-FEB-88
LNL 1987 (CT, BONETTI, FIORETT
BROWN FIELD (iron meteorit
$^{36}Ce/Ce \sim 10^{-12}$
1000
800
600
400
200
0
ΔE_3 —>
0
200
400
600
800
1000
ΔE_1 —>
^{36}S
^{36}Cl

LNL 1987 (luglio) (C.T., Bonetti, Fiorello, ...
BLANK

$^{36}Cl/Cl \sim 10^{-14}$

0.03 cps di ^{36}Cl con 3 μA di ^{35}Cl

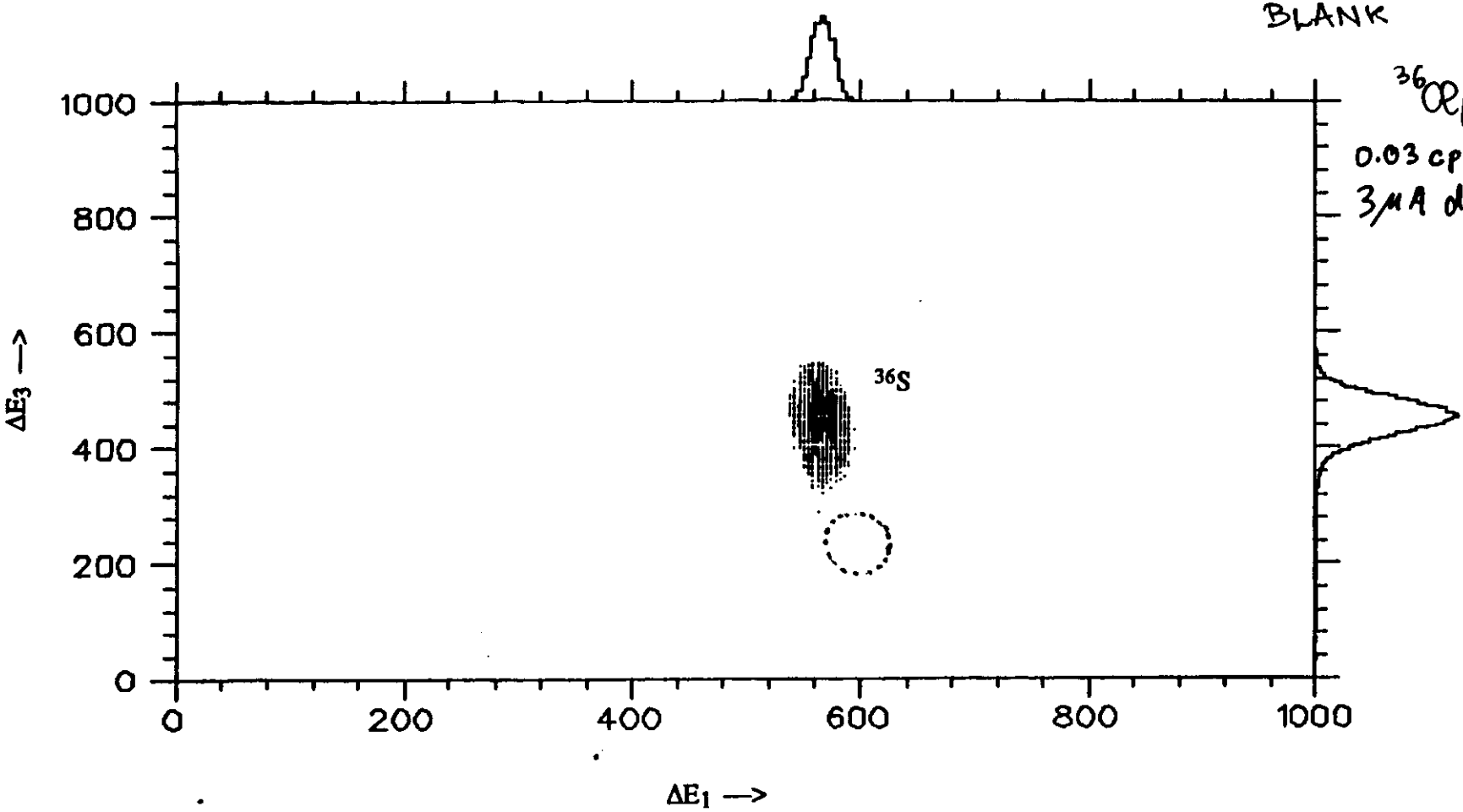

SEARCH FOR RARE PARTICLES AND PROCESSES IN NATURE

I KNOWN PARTICLES PRODUCED IN RARE PROCESSES: SELECTIVE TECHNIQUE (TO MASS, CHARGE, ...)

II HYPOTHETICAL PARTICLES: TECHNIQUE WITH A BROAD RANGE OF PARAMETERS (I.E. MASS OF FREE QUARKS)

AMS SUITABLE FOR I AND II

SEARCH FOR HYPOTHETICAL PARTICLES

1. **PRODUCED WITH ACCELERATORS**
2. **SEARCH IN NATURE**
   - **in cosmic rays**
   - **in ordinary matter**

PROBLEMS: - **LOW CONCENTRATION IN ORDINARY MATTER**

- **WHERE TO SEARCH?**

ORIGINS: - **ANOMALOUSLY HEAVY ISOTOPES**
(heavy charged particles bound to electrons or protons)

- **FRACTIONALLY CHARGED PARTICLES**

(REMNANTS OF THE BIG BANG)

- **SUPERHEAVY ELEMENTS**

(STELLAR EVOLUTION)

CHEMISTRY: **UNKNOWN**

FRACTIONALLY CHARGED PARTICLES (FCP)

THEORY: CONFINEMENT IN HADRONS

EXPERIMENT:
- SUPERCONDUCTING NIOBIUM SPHERES — positive
- ACCELERATORS — negative
- COSMIC RAYS — negative

AMS:
- ARGONNE
- ROCHESTER
- TORONTO
- CALTECH

10^{-18} FCP/NUCLEON

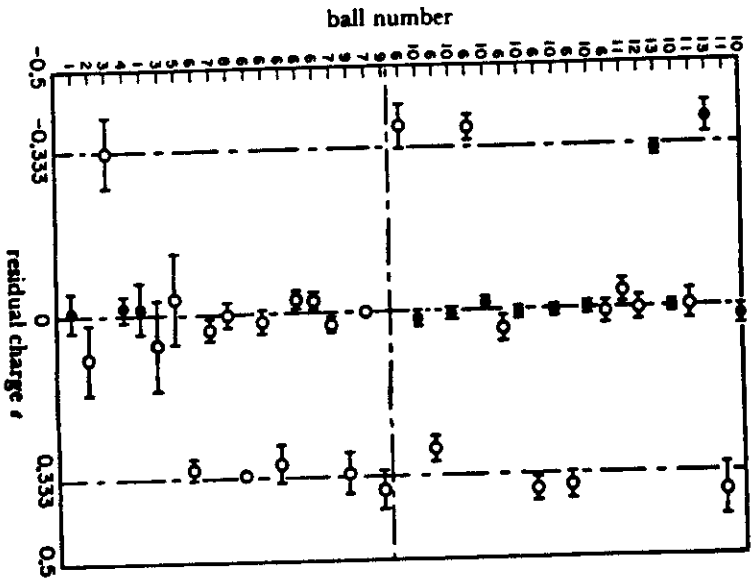

LARUE et al. (1981)

ANOMALOUSLY HEAVY ISOTOPES

THEORY: 10^{-10} - 10^{-12} WOLFRAM (1979); DOVER (1979)

AMS: <<

ARE PRIMORDIAL ABUNDANCIES PRESERVED?

DEPLETION FROM GEOPHYSICS AND GEOCHEMISTRY?

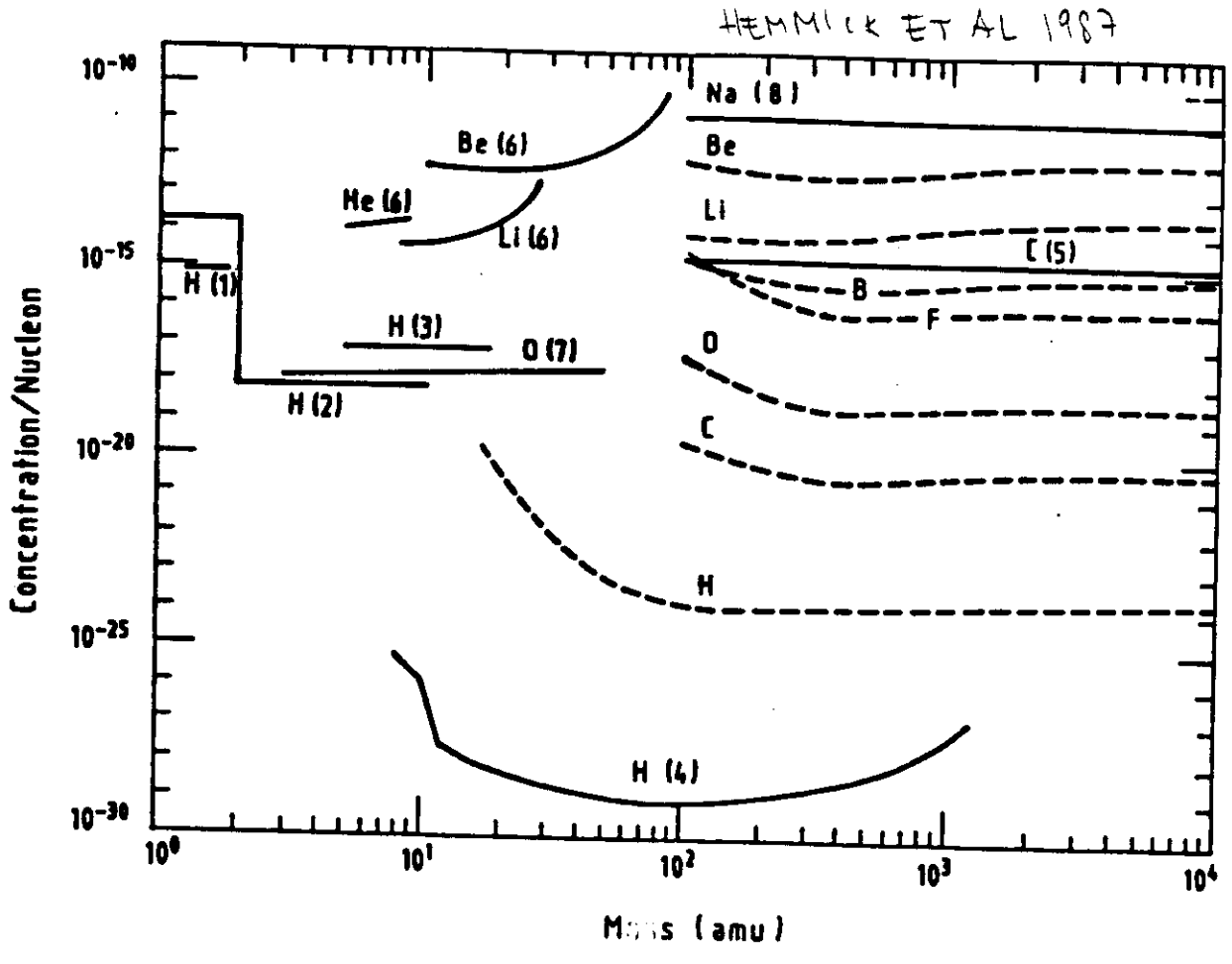

ELMORE
KUBIK
:::

(ROCHESTER)

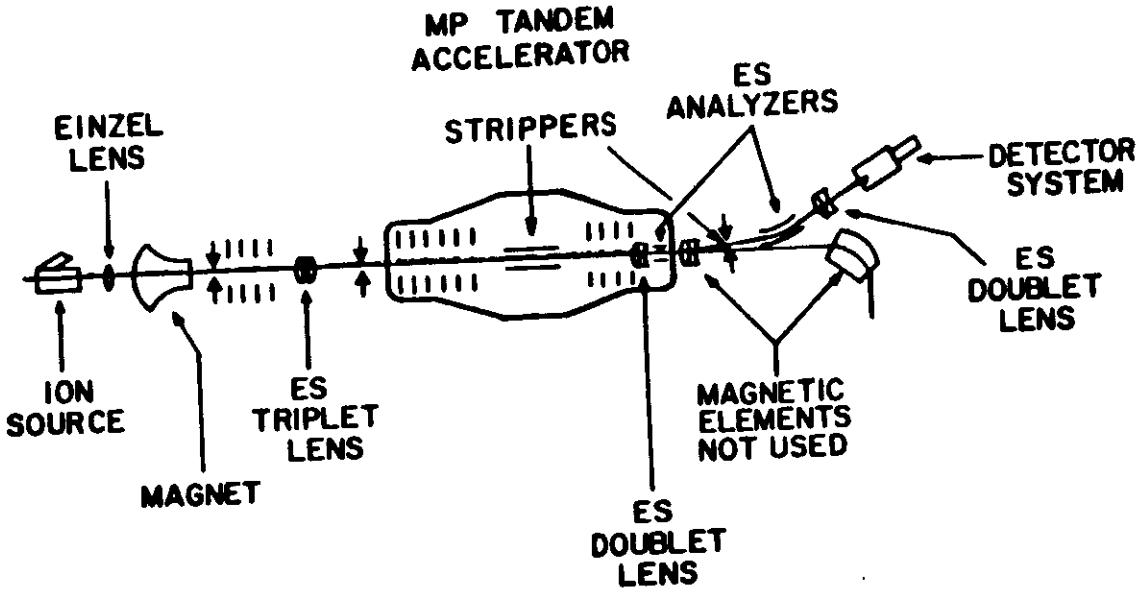

SEARCH FOR:

- FRACTIONALLY CHARGED PARTICLES [10^{-18}]
- ANOMALOUSLY HEAVY PARTICLES

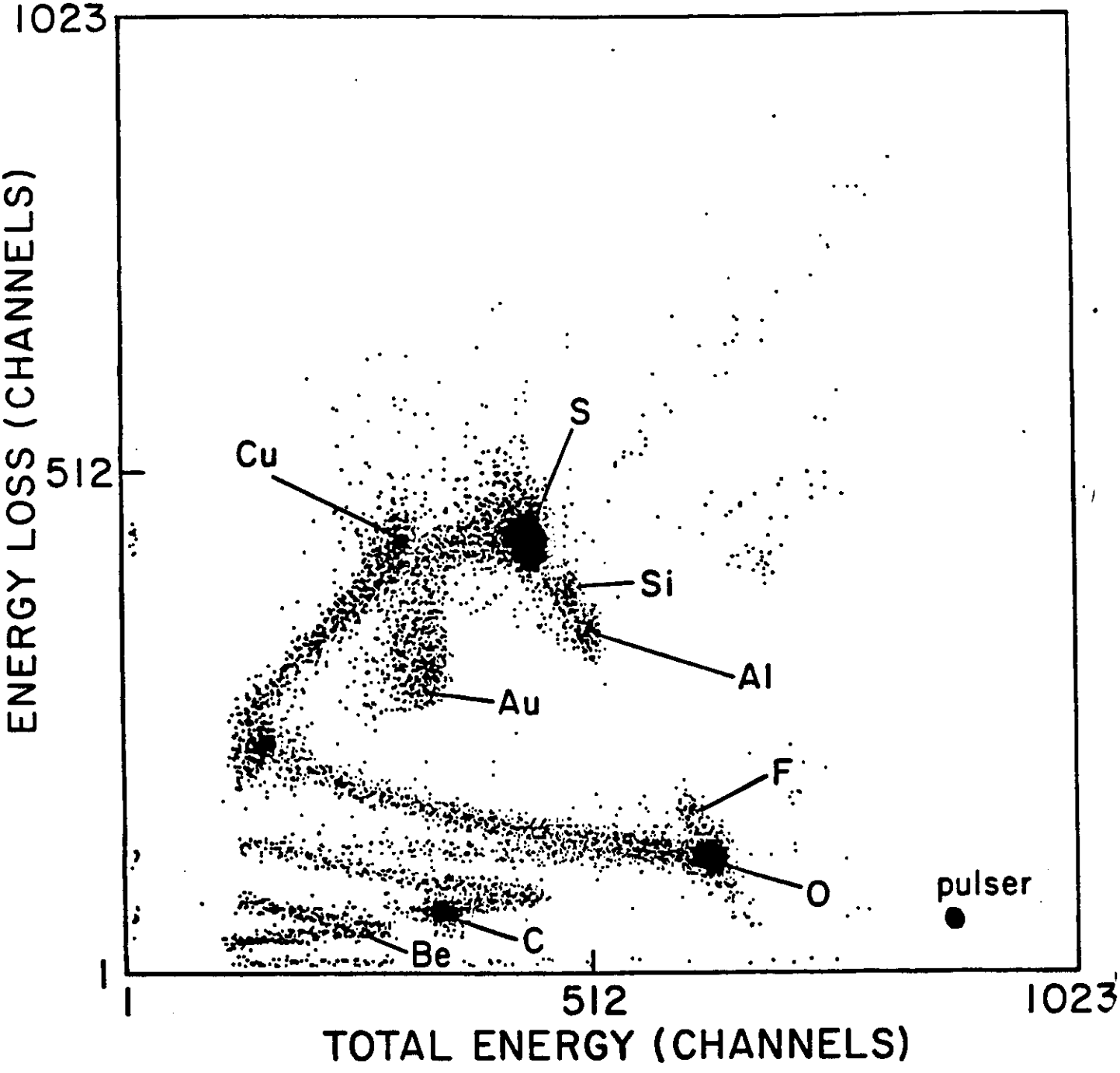

ELMORE ET AL. 1985

Q=1⁻ ; 5 meV ; Q=1⁺

_ STD Be Cu Au

AMS (ROCHESTER)
"AML ELECTROSTATIC"

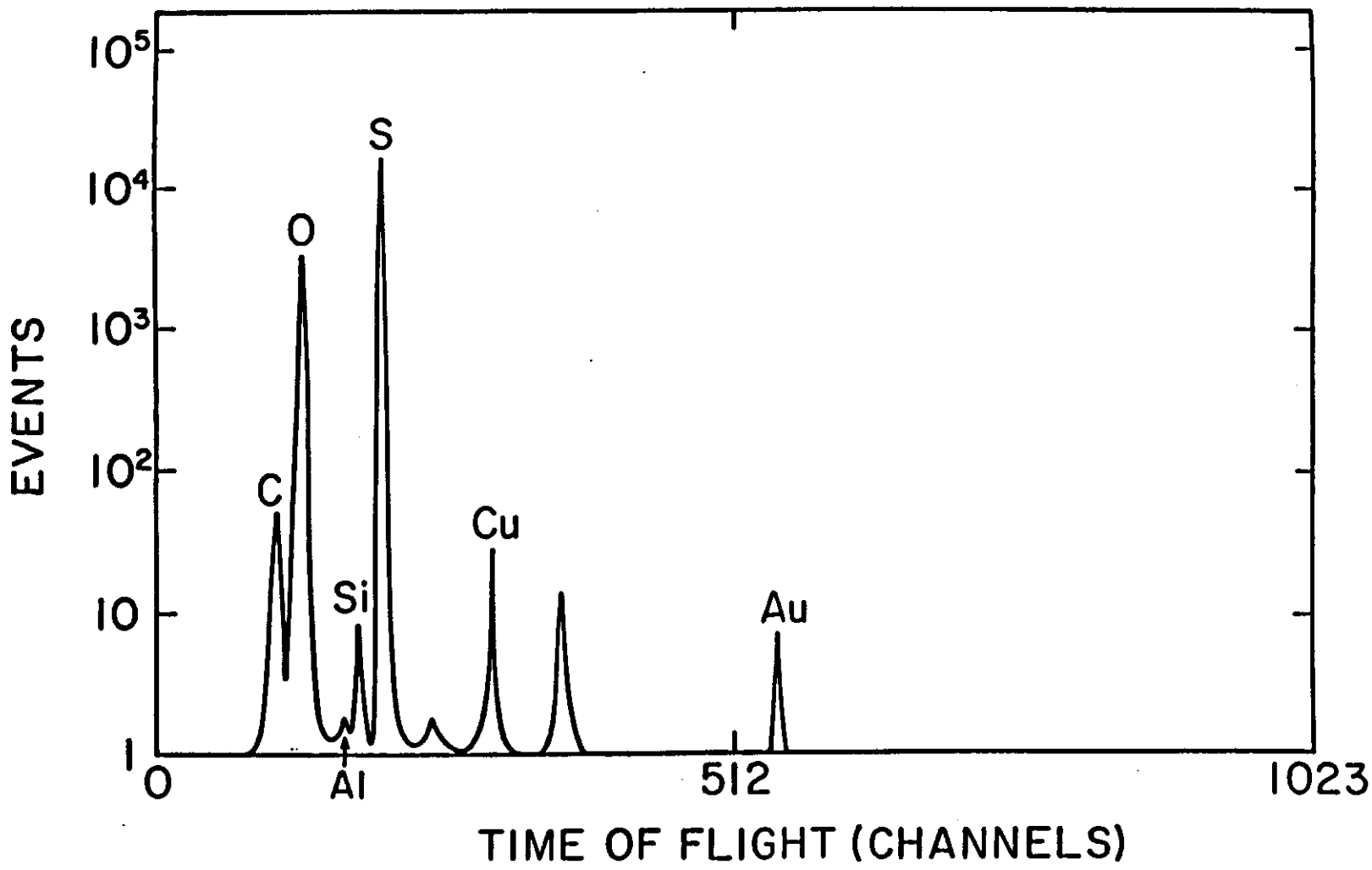

ELMORE ET AL. 1985

RARE PROCESSES:

LOW NUMBER OF ATOMS PRODUCED IN A REASONABLE AMOUNT OF TARGET MATERIAL

PROTON DECAY: ~ 1 event/(10^3 tons.year)

INVERSE BETA DECAY INDUCED BY SOLAR ν's ~ 1 event/(ton . year)

DOUBLE BETA DECAY ~ 1 event/(g . year)

DETECTION OF RARE PROCESSES

1. DIRECT
2. RADIOCHEMICAL
3. <u>GEOCHEMICAL</u>

COMPARE 2. VS 3. FOR SOLAR ν'S

2. $^{37}CL(\nu,e^-)^{37}Ar$

600 tons C_2Cl_4 ($\sim 10^{31}$ atoms)

months ------> 40 ^{37}Ar atoms counted ($t_{1/2}$ = 35 d)

RIS competitive $^{81}Br(\nu,e^-)^{81}Kr$, E_t=0.47 KeV, $T_{1/2}$=0.2 My
months ------> 10^2 atoms (counted directly)

AMS not competitive (?) $^7Li + ? \rightarrow {}^?Be + e^-$

3. AMS efficiency ~ 0.1 %

integration over geological times (10^6 - 10^9 atoms/ton)

problems:
- chemistry
- background from competing reactions
- closedness of the system

THE GEOCHEMICAL METHOD

TO DETECT "RARE" PROCESSES:

- DOUBLE BETA DECAY
- SOLAR NEUTRINOS
- PROTON DECAY

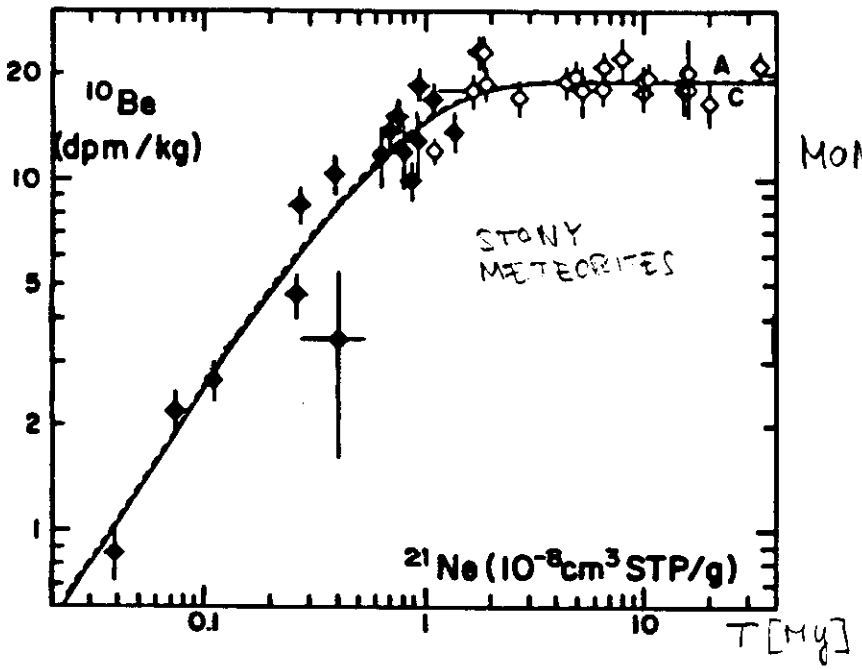

MONIOT, C. T., ...
1984

OTHER APPLICATIONS:

- DATING OF MINERALS (K-Ar)
- COSMIC RAY EXPOSURE AGE OF METEORITES

PRINCIPLE:

- INTEGRAL EFFECT
- GEOLOGICAL TIME
- FINAL PRODUCT COLLECTED IN A CLOSED SYSTEM

EXAMPLE: $\beta\beta$

$\lambda_{\beta\beta} \sim 10^{-21}\ y^{-1}$

medium weight element: ~ 5 events/(g.y)

natural mineral of geological age ($T \sim 10^9$ y)

$\sim 10^9$ product nuclei/g

$$N_D = N_P \cdot \lambda_{\beta\beta} \cdot T \qquad (T \ll \lambda_{\beta\beta}^{-1})$$

T <------- dating of mineral (K-Ar)

N_P <------- chemical analysis

N_D <------ SM, AMS (?)

$$R = i_D/j_D$$

$$(R' - R)/R = \ln 2 \cdot T/T_{1/2} \cdot [P]/[J_D] \cdot I(i_P)/(I(i_D)/I(j_D))$$

SM 10^{-5}	10^{-12}	10^{7}
AMS 10^{-2}	10^{-12}	10^{10}

MAIN PROBLEM: PRIMORDIAL CONTAMINATION

SOLUTION: - FINAL PRODUCT RADIOACTIVE

- FINAL PRODUCT A NOBLE GAS

- GEOCHEMICAL FRACTIONATION

SECOND PROBLEM: COUNTING A "SMALL" NUMBER OF NUCLEI IN A "SEA" OF OTHER ATOMS (isotopic abundances 10^{-10} - 10^{-20})

SOLUTION:
- MASS SPECTROMETRY
- AMS
- RIS
- RIS + AMS

"SOLAR NEUTRINO PUZZLE"

STANDARD SOLAR MODEL
(Bahcall)

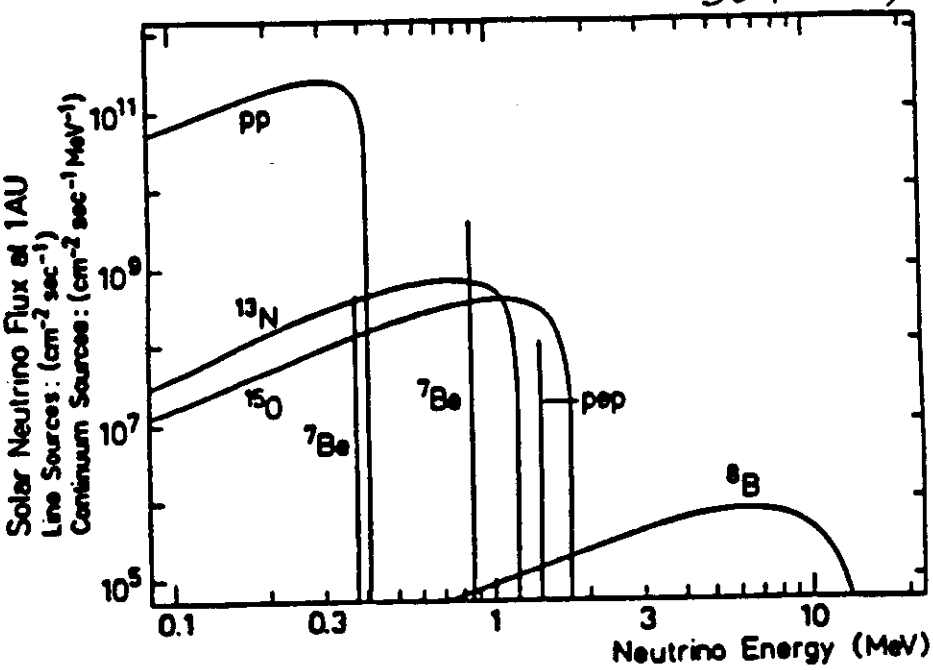

DISCREPANZA CON ESPERIMENTO "RADIOCHIMICO"
[DAVIS et al.]

$$\nu + {}^{37}Cl \longrightarrow {}^{37}Ar + e^-$$

SORGENTI DI NEUTRINI ED ENERGIE (MeV)	FLUSSO SULLA TERRA Φ ($cm^{-2}\,sec^{-1}$)	σ (cm^2)	RATE CATTURA NEL ^{37}Cl $\Phi\sigma \times 10^{36}$ (SNU)
$H+H \rightarrow D+e^+ +\nu$ (0-0.42)	6.1×10^{10}	0	0
$H+H+e^- \longrightarrow D+\nu$ (1.44)	1.5×10^{8}	1.54×10^{-45}	0.23
$^7Be+e^- \longrightarrow {}^7Li+\nu$ (0.86 [89.6%] / 0.384 [10.4%])	3.4×10^{9}	2.4×10^{-46}	0.80
$^8B \longrightarrow {}^8Be+e^+ +\nu$ (0-14)	3.2×10^{6}	1.08×10^{-42}	3.46
$^{15}O \rightarrow {}^{15}N+e^+ +\nu$ (0-1.74)	1.8×10^{8}	6.6×10^{-46}	0,12
$^{13}N \rightarrow {}^{13}C+e^+ +\nu$ (0-1.19)	2.6×10^{8}	1.6×10^{-46}	0.04
			$\Sigma\Phi\sigma = 4.65$

EXP.: 1.6 ± 0.4 SNU

REAZIONI NUCLEARI NEL SOLE:

CATENA p-p

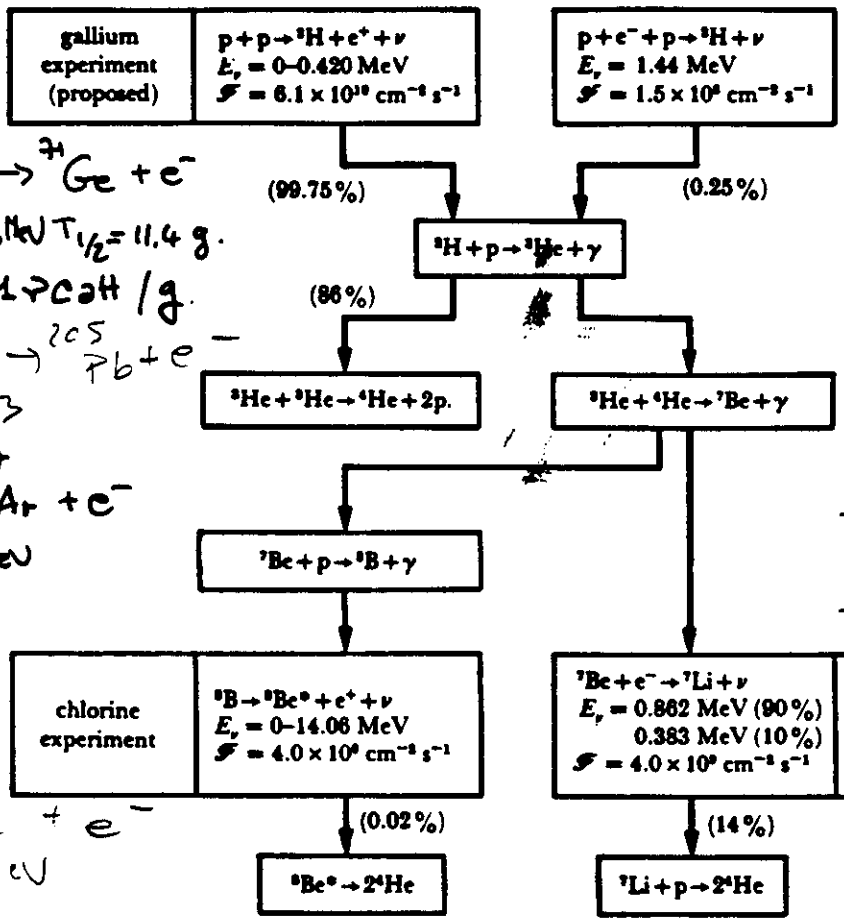

$\nu + {}^{71}Ga \longrightarrow {}^{71}Ge + e^-$

$E_s = 0.233$ MeV $T_{1/2} = 11.4$ g.

38 ton: 1 Cell / g.

$\nu + {}^{205}Tl \rightarrow {}^{205}Pb + e^-$

$E_s = 0.043$

$\nu + {}^{37}Cl \rightarrow {}^{37}Ar + e^-$

$E_s = 0.82$ MeV

$T_{1/2} = 35$ g.

$\nu + {}^{81}Br \rightarrow {}^{81}Kr + e^-$

$E_s = 0.47$ MeV

$T_{1/2} = 2.1 \times 10^5$ a.

$\nu + {}^{99}Mo \rightarrow {}^{99}Tc + e^-$

$E_s = 1.5$ MeV

$\nu + {}^{41}K \rightarrow e^- + {}^{41}Ca$

$E_T = 2.6$ MeV

CICLO C-N-O

$${}^{12}C + {}^{1}H \longrightarrow {}^{13}N + \gamma$$
$${}^{13}N \longrightarrow {}^{13}C + e^+ + \nu$$
$${}^{13}C + {}^{1}H \longrightarrow {}^{14}N + \gamma$$
$${}^{14}N + {}^{1}H \longrightarrow {}^{15}O + \gamma$$
$${}^{15}O \longrightarrow {}^{15}N + e^+ + \nu$$
$${}^{15}N + {}^{1}H \longrightarrow {}^{12}C + {}^{4}He$$

run nos	production rate (^{37}Ar per day) most likely value	68% confidence range
18→39	0.38	0.31–0.46
40→47	0.39	0.27–0.50
18→47	0.38	0.33–0.45

average ^{37}Ar production rate (18→47) = 0.38±0.07
cosmic-ray background (muons and ν_μ) = 0.06±0.03

rate above known backgrounds = 0.30±0.08

Possible solar-neutrino rate = 5.24 × (0.30±0.08) = 1.6±0.4 SNU.

$\nu + {}^{41}K \text{ -------> } e^- + {}^{41}Ca$

^{41}K: 6.73 %
$T_{1/2} = 1.3 \times 10^5$ y
$E_T = 2.43$ MeV
(only ν from ^8B)

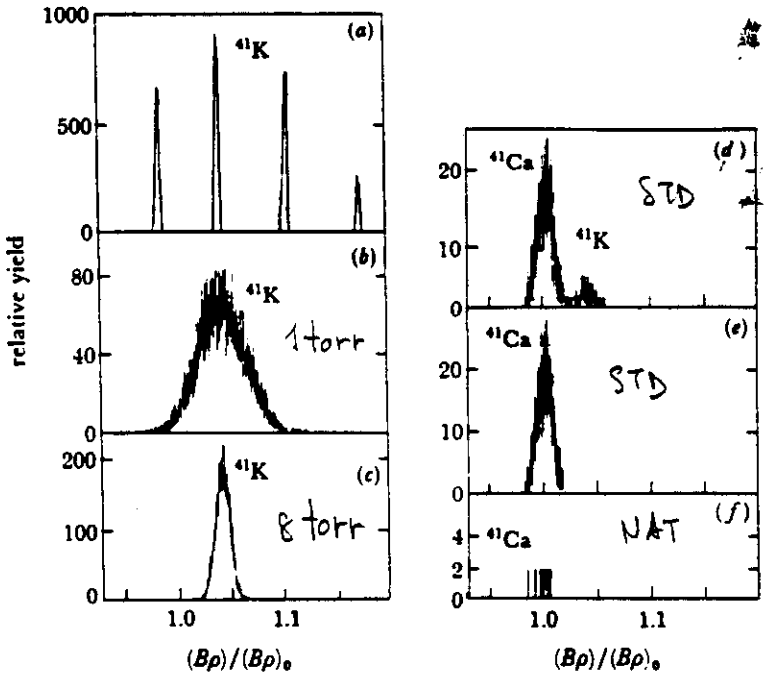

G. Korshinek et al. 1987
TANDEM + POSTACC.
(MUNICH) - 5.5 MeV/AMU
$^{41}Ca/Ca = 9 \times 10^{-12}$

W. Henning et al. 1987
TANDEM + LINAC
(ARGONNE) - 7 MeV/AMU
- $^{41}CaH_3^-$
- gas filled magnetic spec.
$^{41}Ca/Ca = 6 \times 10^{-14}$

Steinhof et al. 1987
UNILAC (GSI) - 14 MeV/AMU
$^{41}Ca/Ca = 2 \times 10^{-14}$

HAXTON (1980): 7.7 +/- 0.3 SNU

background from μ: < 10% [1500 m depth]

background from (n,γ) and (α,n): < 10% [U and Th < ppm]

KCl deposit Regina (Saskatchewan)

1.3 tons of KCl ------> 1 kg Ca ------> 10^4 ^{41}Ca atoms

AMS: 10 mg
10^5 enrichment necessary
or
@ equilibrium: $^{41}Ca/^{41}K = 4 \times 10^{-25}$

$^{40}Ca/^{41}K = 10^{-4}$

10^5 enrichment to get $^{41}Ca/^{40}Ca = 10^{-16}$

$\nu + {}^{205}Tl$ ------> $e^- + {}^{205}Pb^m$ (2.3 keV) $T_{1/2}$ =1.6 My

^{205}Tl: 70.9 %

----> ^{205}Pb E_t = 0.048 MeV

(it includes νfrom p-p)

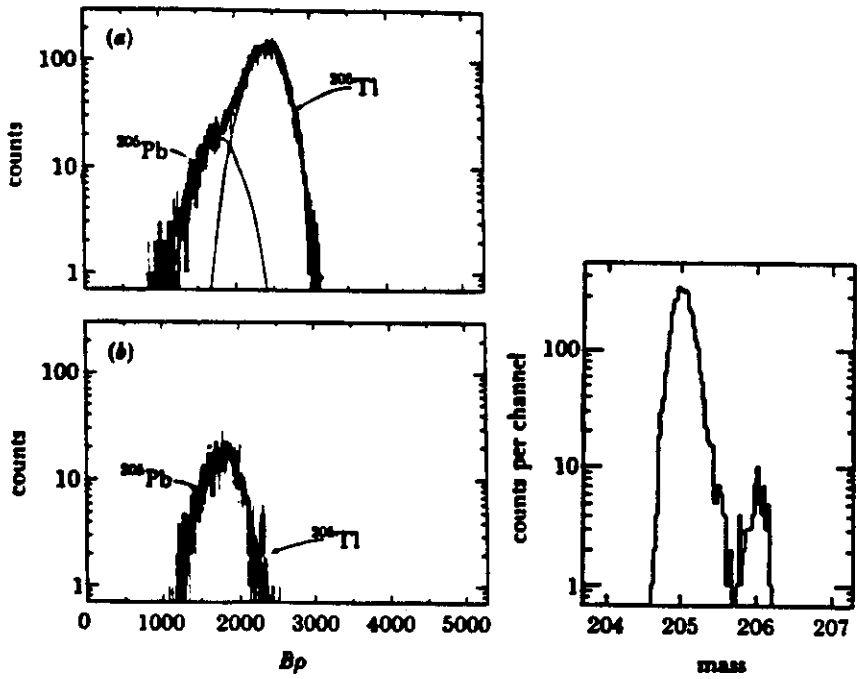

Henning et al.(1987)
UNILAC @ GSI
$Q=29^+$; 2.3 GeV

Isotopic separation: OK
Source efficiency: NO

FREEDMAN ET AL. (1976): 430 +/-100 SNU
(85% FROM p-p)

"LORANDITE" ($TlAsS_2$), MACEDONIA, YUGOSLAVIA

T=10 My
Pb: 3 ppm

20 TONS ----> 100 KG LORANDITE ----> 10^7 ^{205}Pb ATOMS

@ equilibrium: $^{205}Pb/Pb = 10^{-13} - 10^{-14}$

$^{205}Pb/^{205}Tl = 3x10^{-19}$

- ISOTOPIC SEPARATION: OK
- ISOBARIC SEPARATION ($Tl/Pb \leq 10^{-11}$)
- PROBLEM: SOURCE EFFICIENCY (10^{-6}) ⟶ (1%)

Pb^{9+}

Table 1 $\beta^-\beta^-$ decay transitions for naturally occurring parent isotopes*

Transition	T_0 (keV)	Abundance (%)	Excitation energy of first 2^+ state (keV)**
$^{46}Ca \rightarrow {}^{46}Ti$	985	0.0035	889
$^{48}Ca \rightarrow {}^{48}Ti$†	4272	0.187	984
$^{70}Zn \rightarrow {}^{70}Ge$	1001	0.62	—
$^{76}Ge \rightarrow {}^{76}Se$	2045	7.8	559
$^{80}Se \rightarrow {}^{80}Kr$	136	49.8	—
$^{82}Se \rightarrow {}^{82}Kr$	3005	9.2	776
$^{86}Kr \rightarrow {}^{86}Sr$	1249	17.3	1077
$^{94}Zr \rightarrow {}^{94}Mo$	1148	17.4	871
$^{96}Zr \rightarrow {}^{96}Mo$†	3350 –	2.8	778
$^{98}Mr \rightarrow {}^{98}Ru$	111	24.1	—
$^{100}Mo \rightarrow {}^{100}Ru$	3033	9.6	540
$^{104}Ru \rightarrow {}^{104}Pd$	1301	18.7	556
$^{110}Pd \rightarrow {}^{110}Cd$	2014	11.8	658
$^{114}Cd \rightarrow {}^{114}Sn$	540	28.7	—
$^{116}Cd \rightarrow {}^{116}Sn$	2808	7.5	1294
$^{122}Sn \rightarrow {}^{122}Te$	358	4.56	—
$^{124}Sn \rightarrow {}^{124}Te$	2278	5.64	603
$^{128}Te \rightarrow {}^{128}Xe$	869	31.7	443
$^{130}Te \rightarrow {}^{130}Xe$	2533	34.5	536
$^{134}Xe \rightarrow {}^{134}Ba$	843	10.4	605
$^{136}Xe \rightarrow {}^{136}Ba$	2481	8.9	819
$^{142}Ce \rightarrow {}^{142}Nd$	1414	11.1	—
$^{146}Nd \rightarrow {}^{146}Sm$‡	61	17.2	—
$^{148}Nd \rightarrow {}^{148}Sm$	1928	5.7	550
$^{150}Nd \rightarrow {}^{150}Sm$	3367	5.6	334
$^{154}Sm \rightarrow {}^{154}Gd$	1250	22.6	123
$^{160}Gd \rightarrow {}^{160}Dy$	1731	21.8	87
$^{170}Er \rightarrow {}^{170}Yb$	655	14.9	84
$^{176}Yb \rightarrow {}^{176}Hf$	1077	12.6	88
$^{186}W \rightarrow {}^{186}Os$	489	28.6	137
$^{192}Os \rightarrow {}^{192}Pt$	408	41.0	317
$^{198}Pt \rightarrow {}^{198}Hg$	1043	7.2	412
$^{204}Hg \rightarrow {}^{204}Pb$	414	6.9	—
$^{232}Th \rightarrow {}^{232}U$§	850	100	48
$^{238}U \rightarrow {}^{238}Pu$¶	1146	99.275	44

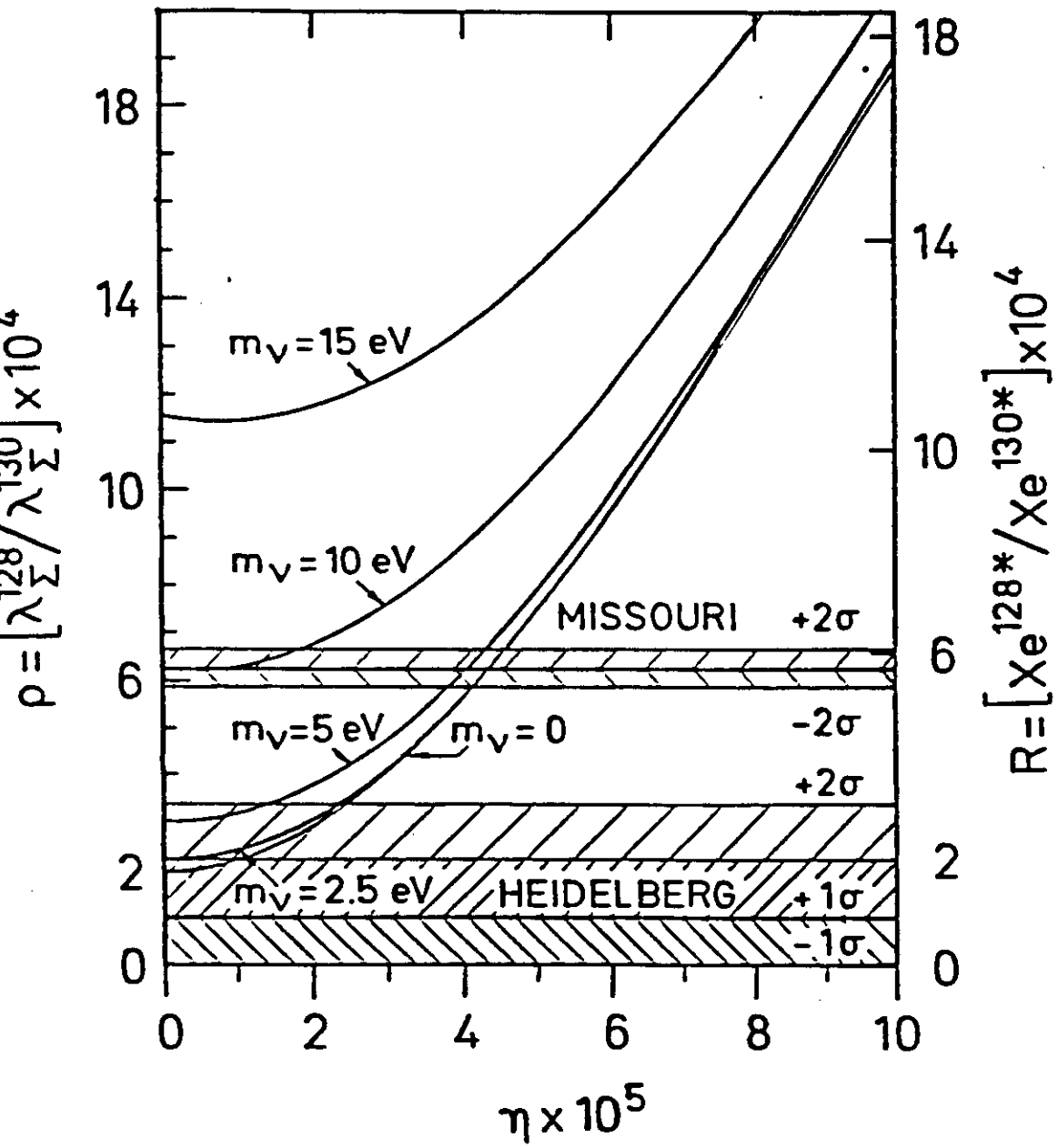
$\rho = [\lambda_{\Sigma}^{128}/\lambda_{\Sigma}^{130}] \times 10^4$
$R = [Xe^{128*}/Xe^{130*}] \times 10^4$
$\eta \times 10^5$
$m_\nu = 15$ eV
$m_\nu = 10$ eV
$m_\nu = 5$ eV
$m_\nu = 0$
$m_\nu = 2.5$ eV
MISSOURI
HEIDELBERG
$+2\sigma$
-2σ
$+2\sigma$
$+1\sigma$
-1σ
0
2
4
6
8
10
0
2
6
10
14
18

KIRSTEN

KIRSTEN

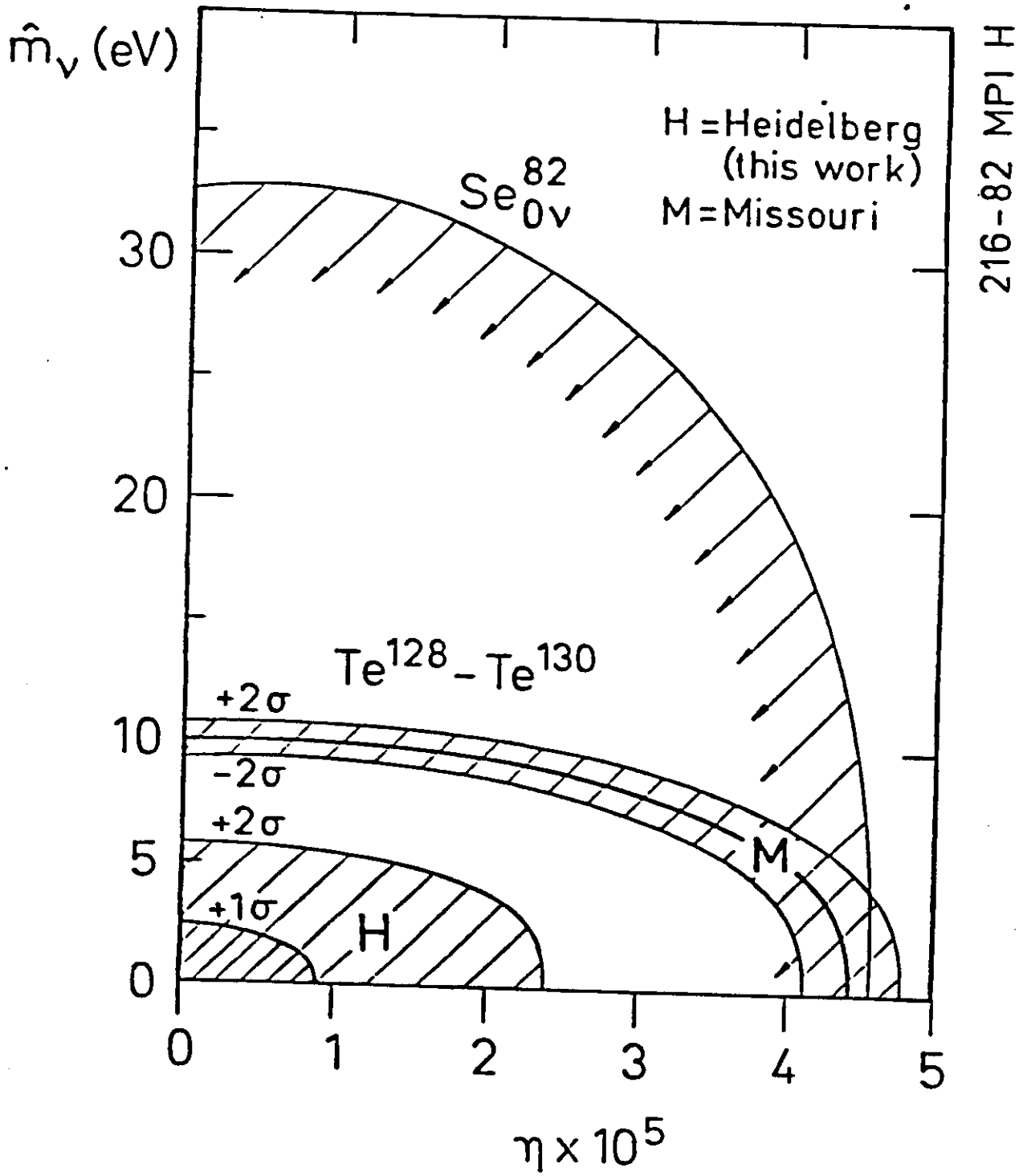
$\hat{m}_\nu$ (eV)
H = Heidelberg (this work)
M = Missouri
$Se^{82}_{0\nu}$
$Te^{128} - Te^{130}$
+2σ
-2σ
+2σ
+1σ
H
M
0
5
10
20
30
0
1
2
3
4
5
$\eta \times 10^5$
216-82 MPI H

$^{96}Zr(\beta\beta)^{96}Zr$

1 Mg Zr

$T_{1/2}^{2\nu} = 3.2 \times 10^{18}$ y

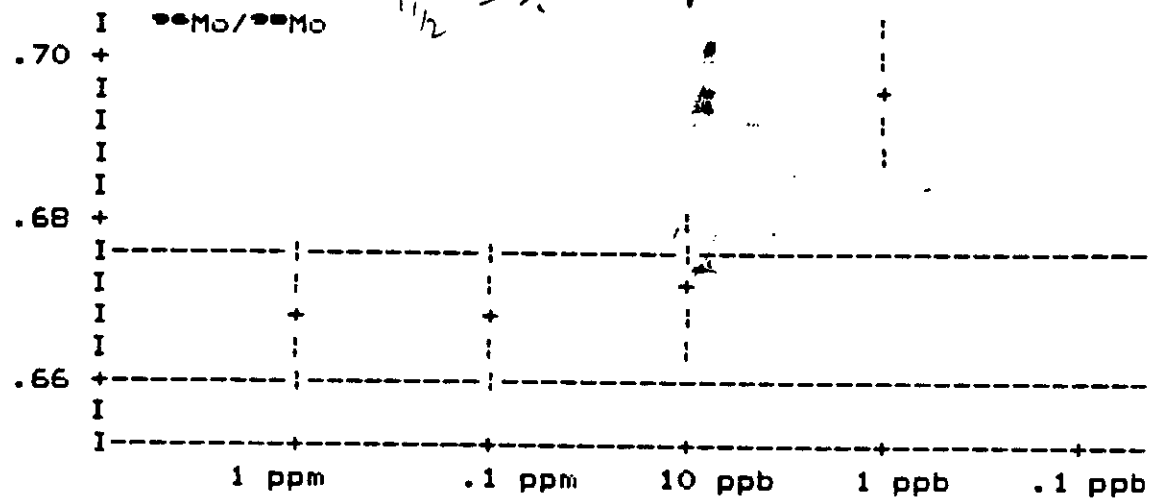

PRIMORDIALE M_o

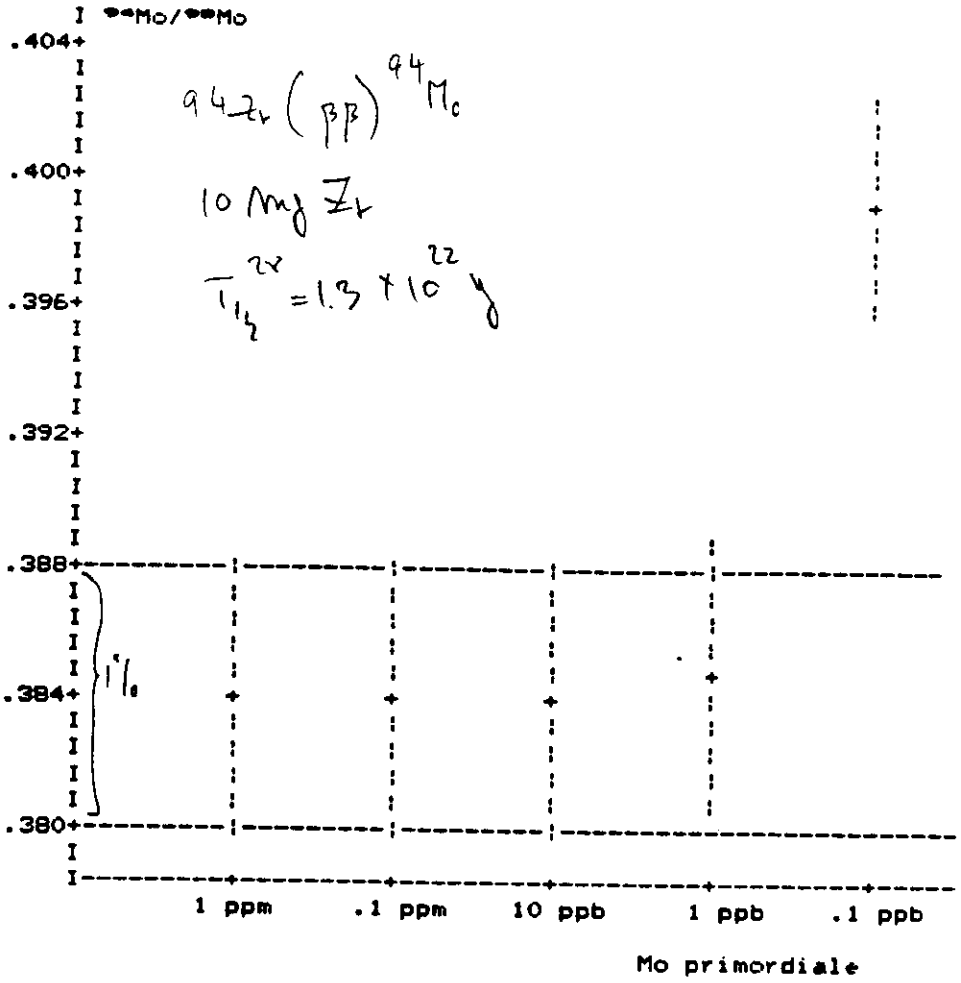

$^{94}Zr(\beta\beta)^{94}Mo$

10 Mg Zr

$T_{1/2}^{2\nu} = 1.3 \times 10^{22}$ y

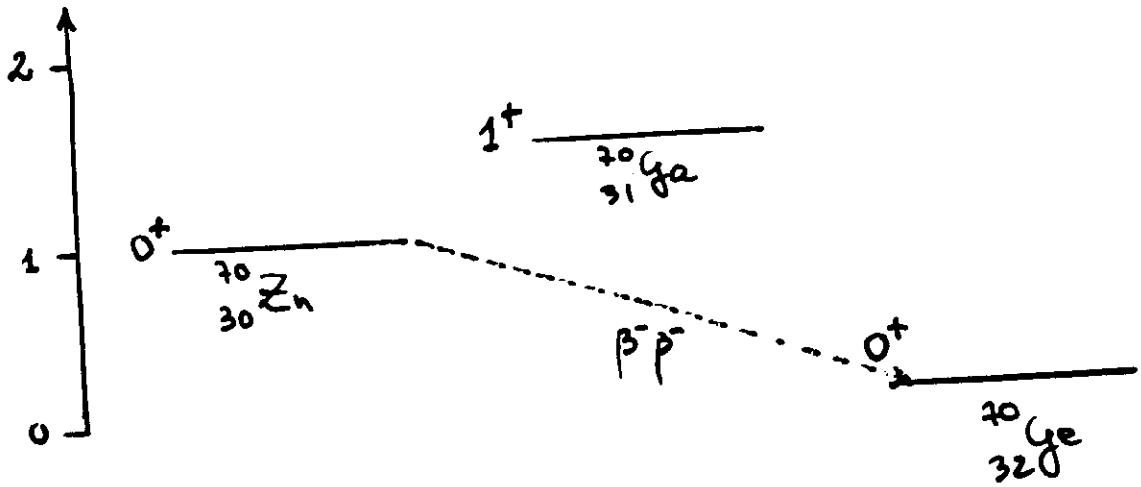

$(\beta\beta)_{2\nu}$

- $(A,Z) \rightarrow (A,Z+2) + e^- + e^- + \bar{\nu}_e + \bar{\nu}_e$

$\langle \tau_{2\nu} \rangle \sim \underset{\text{mmm}}{10}^{23\pm2}\ yr \left(\frac{1\,MeV}{T_0}\right)^8$ [*]

$\lambda_{2\nu} = (\text{Kinem. factor}) \left| M_{GT}^{2\nu} \right|^2$

$T_{1/2}^{2\nu}\left(^{70}_{30}Zn \longrightarrow ^{70}_{32}Ge\right) > 10^{23}\ yr$ [**]

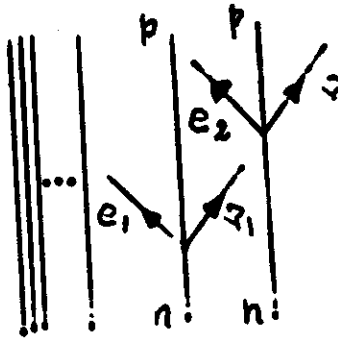

DIRAC

A-2 nucleons

$(\beta\beta)_{0\nu}$

- $(A,Z) \rightarrow (A,Z+2) + e^- + e^-$

$\langle \tau_{0\nu} \rangle \sim \underset{\text{mmm}}{10}^{15\pm2} / \left\{ (m_\nu/m_e)^2 + \eta^2 \right\}$ [*]

$\lambda_{0\nu} = (\text{Kinem. factor}) \cdot \left| M_{GT}^{0\nu} \right|^2 \cdot f(m_\nu, \eta)$

$\tau_{exp} \sim 10^{22} \Longrightarrow \eta$ or $\frac{m_\nu}{m_e} \sim 10^{-5}$

η: $\frac{V+A\ \text{current}}{V-A\ \text{current}}$

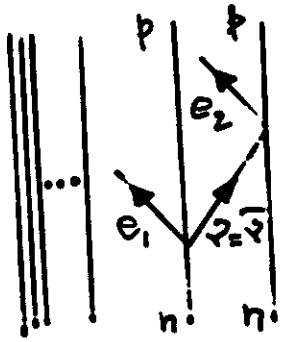

MAJORAN

[*] EXPERIMENTAL PARTICLE PHYSICS WITHOUT ACCELERATORS
[PHYS. REP., 151 (1987) 240

[**] HAXTON et al. 1984

SAMPLE: 100 mg Zn [SPHALERITE]

$T_G = 1.8 \times 10^9$ yr

$Ge^B = f\ Zn$ $\quad f = ?$ {ion source / mineral}

$$\pi = \frac{^{70}Ge^B + {}^{70}Ge^{\beta\beta}}{^{74}Ge^B} = \pi_0 + \frac{^{70}Ge^{\beta\beta}}{^{74}Ge^B}$$

$$^{70}Ge \simeq {}^{70}Zn \cdot T$$

$\pi_0 = 0.559$

$$\Delta\pi = \pi - \pi_0 = 3.2 \times 10^7 \times \frac{\lambda^{\beta\beta}}{f}$$

ex 1:	$T_{1/2}^{\beta\beta}$ [yr]	f	$\Delta\pi$	$\Delta\pi/\pi_0$
	10^{21}	10^{-12}	0.022	4 %
	10^{18}	10^{-9}	0.022	4 %

ex.2: $T_{1/2}^{\beta\beta} = 10^{21}$ yr ; $f = 10^{-12}$; tot. eff.: 0.001 [from source to detector]

	100 mg SAMPLE	DETECTOR [hours]
^{70}Zn	$\sim 10^{19}$ atoms	$\sim 10^4$ counts
$^{70}Ge^B$	$\sim 10^8$ "	$\sim 10^5$ "
$^{70}Ge^{\beta\beta}$	$\sim 10^7$ "	$\sim 10^4$ "
$^{72}Ge^B$	$\sim 10^8$ "	$\sim 10^5$
$^{74}Ge^B$	$\sim 10^8$ "	$\sim 10^5$

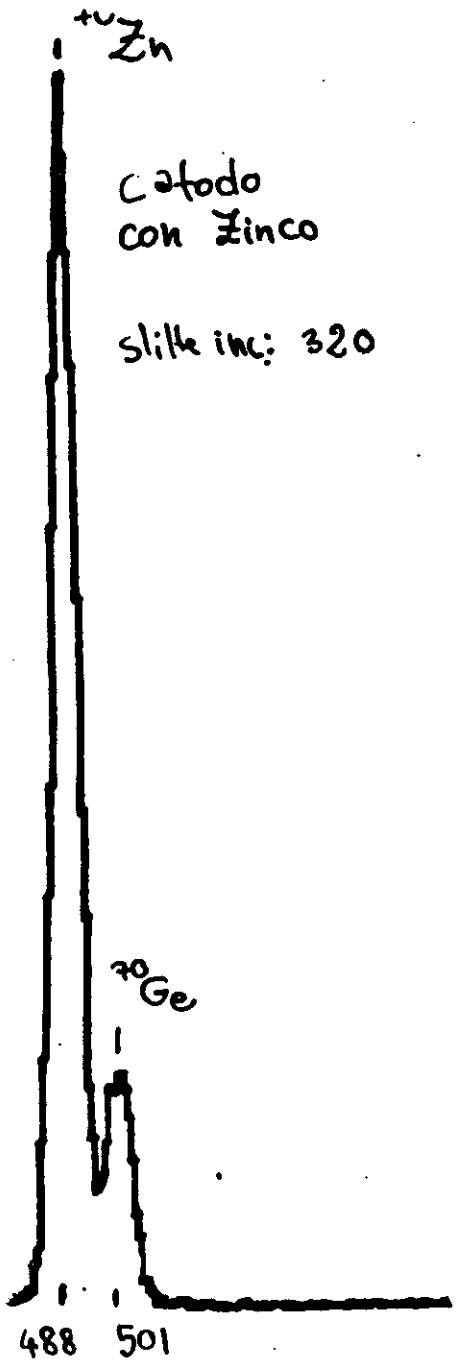

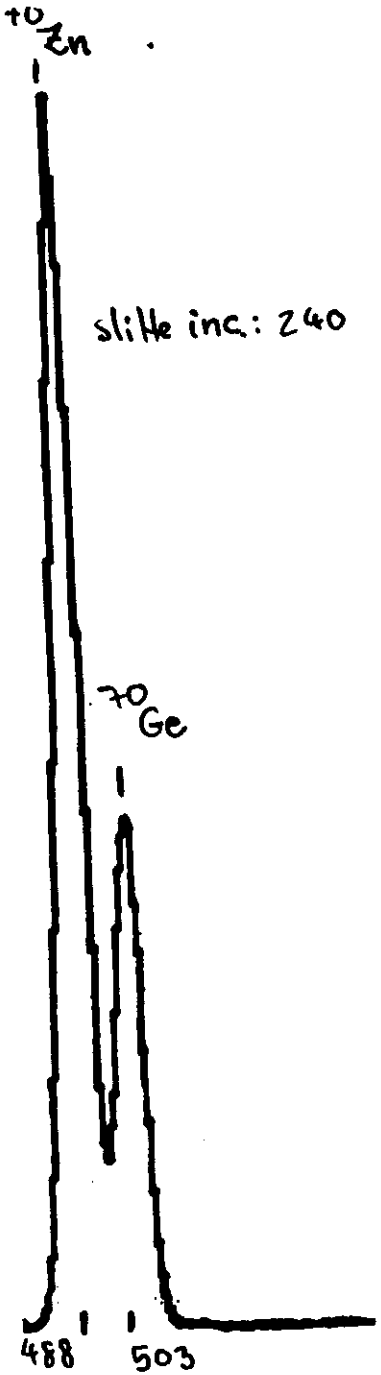

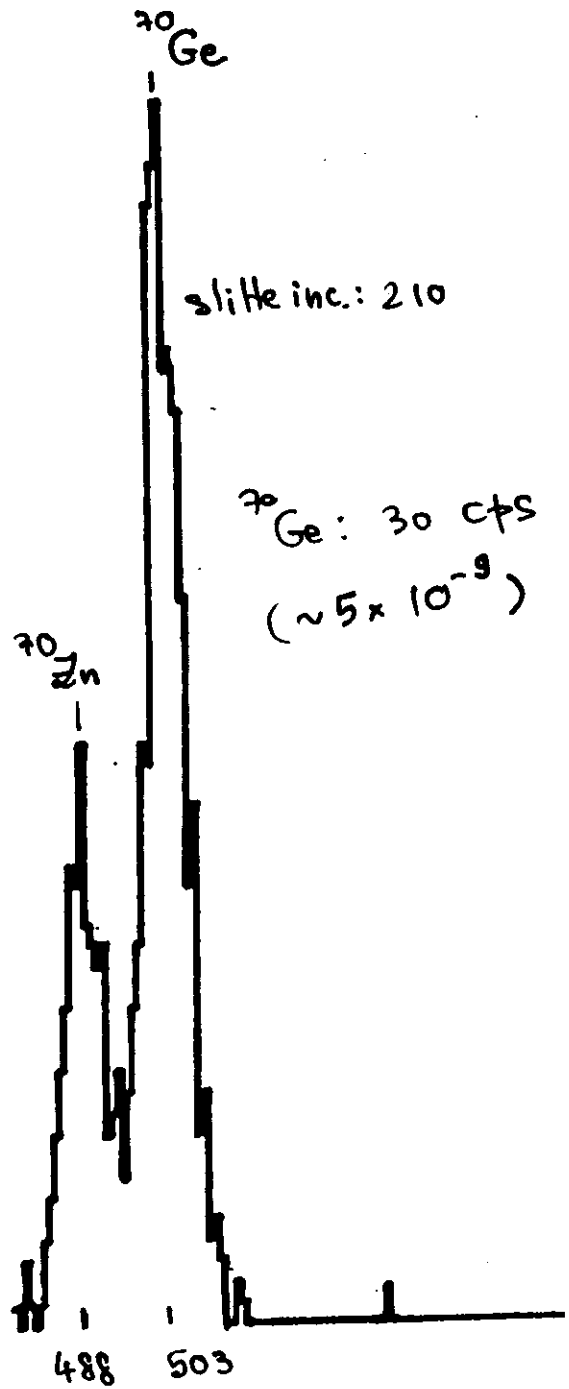

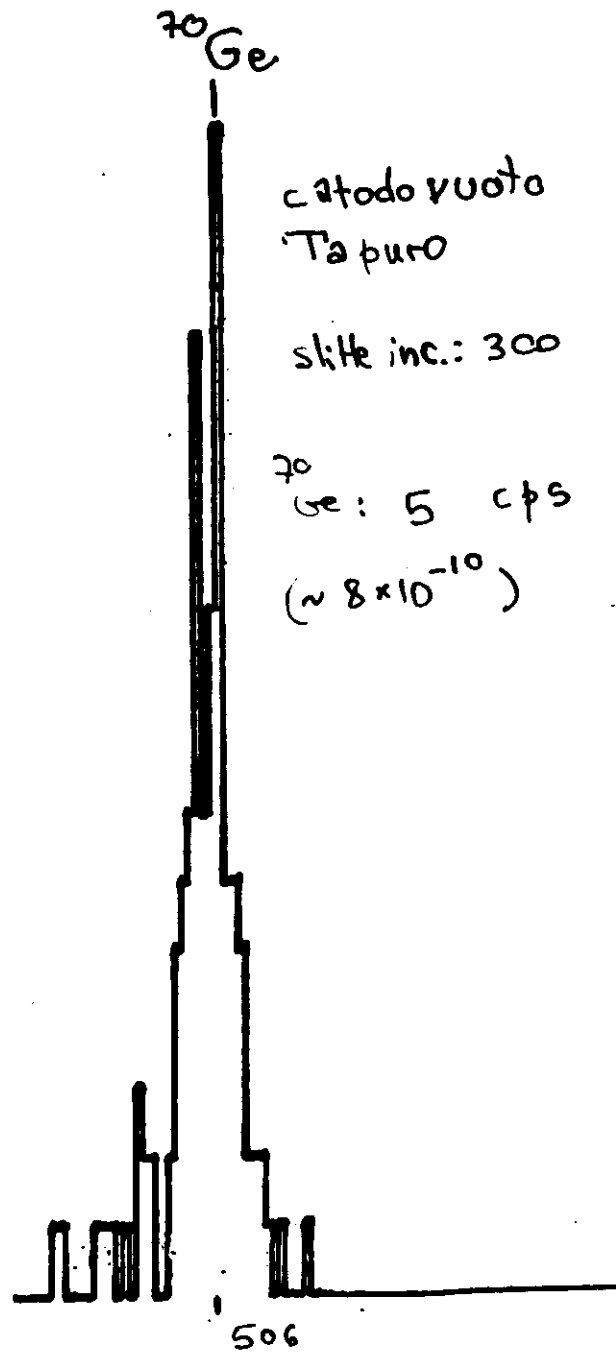

TS-LNL-M1 22 DIC 1987

[Bragg pea

TUNIZ, FINK, SHARMA
MIDDLETON, KLEIN
26-27 OCT 87

U. of PENNA
8 MV
9+

Wien filter: ±48 KV

100SEC. ~~2N CATHODE~~ SOUCE SLITS OPEN, 70ZN 6KHZ AT 70.1, 2N/GE=2.15
ARRAY:: 102 GE2N70S102.270C87
X-AXIS:: X CHANNELS 0 TO 63 OUT OF 64
Y-AXIS:: YY CHANNELS 0 TO 63 OUT OF 64
LOGARITHMIC BASE = 2.00

012...9

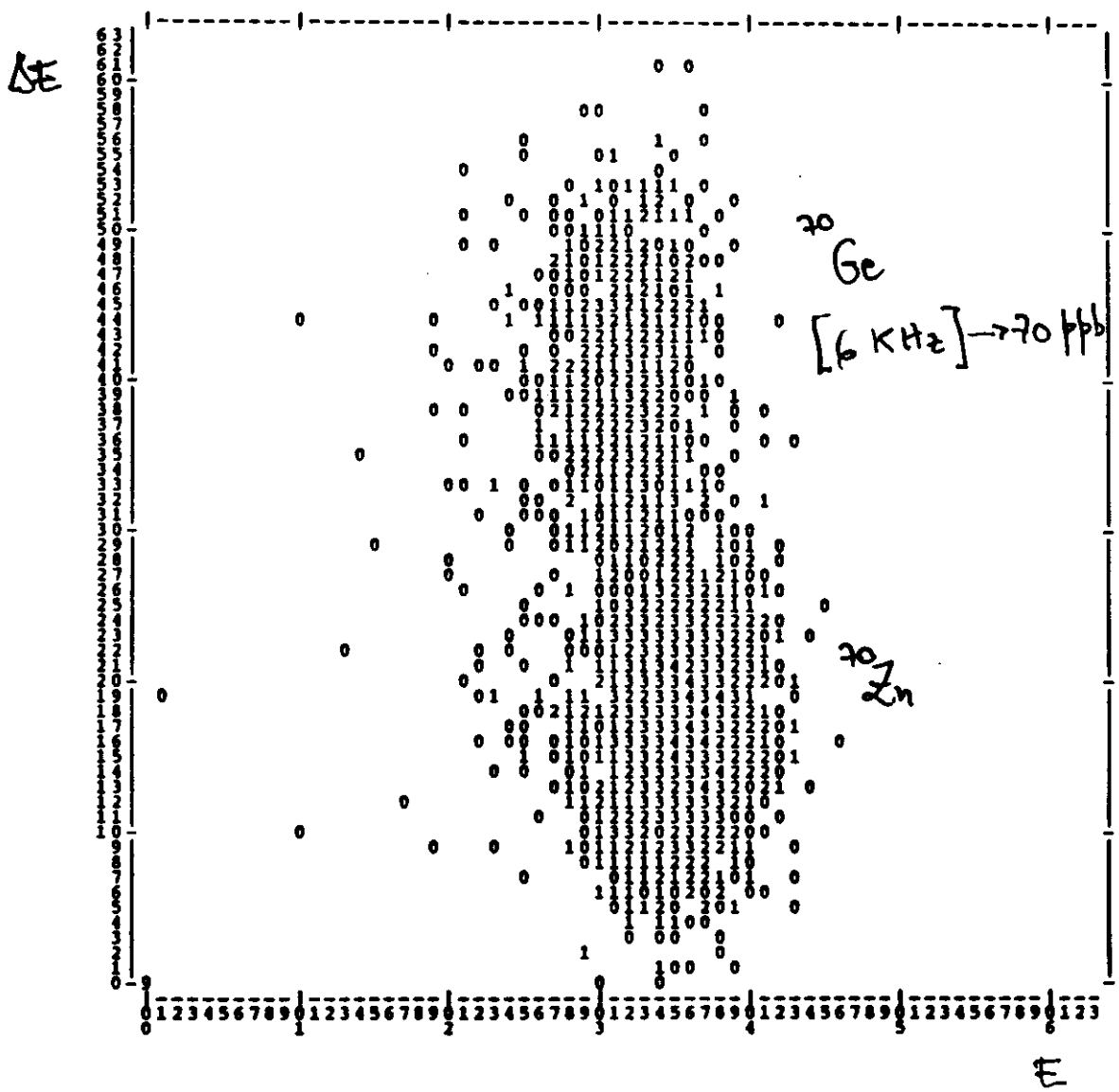

10SEC ZN SOURCE SLITS CLOSED, SOURCE AT 12MA
ARRAY: 1D2 GLEN7010 27OCT87
X-AXIS: XX CHANNELS 0 TO 63 OUT OF 64
Y-AXIS: YY CHANNELS 0 TO 63 OUT OF 64
LOGARITHMIC BASE = 2.00

012...9

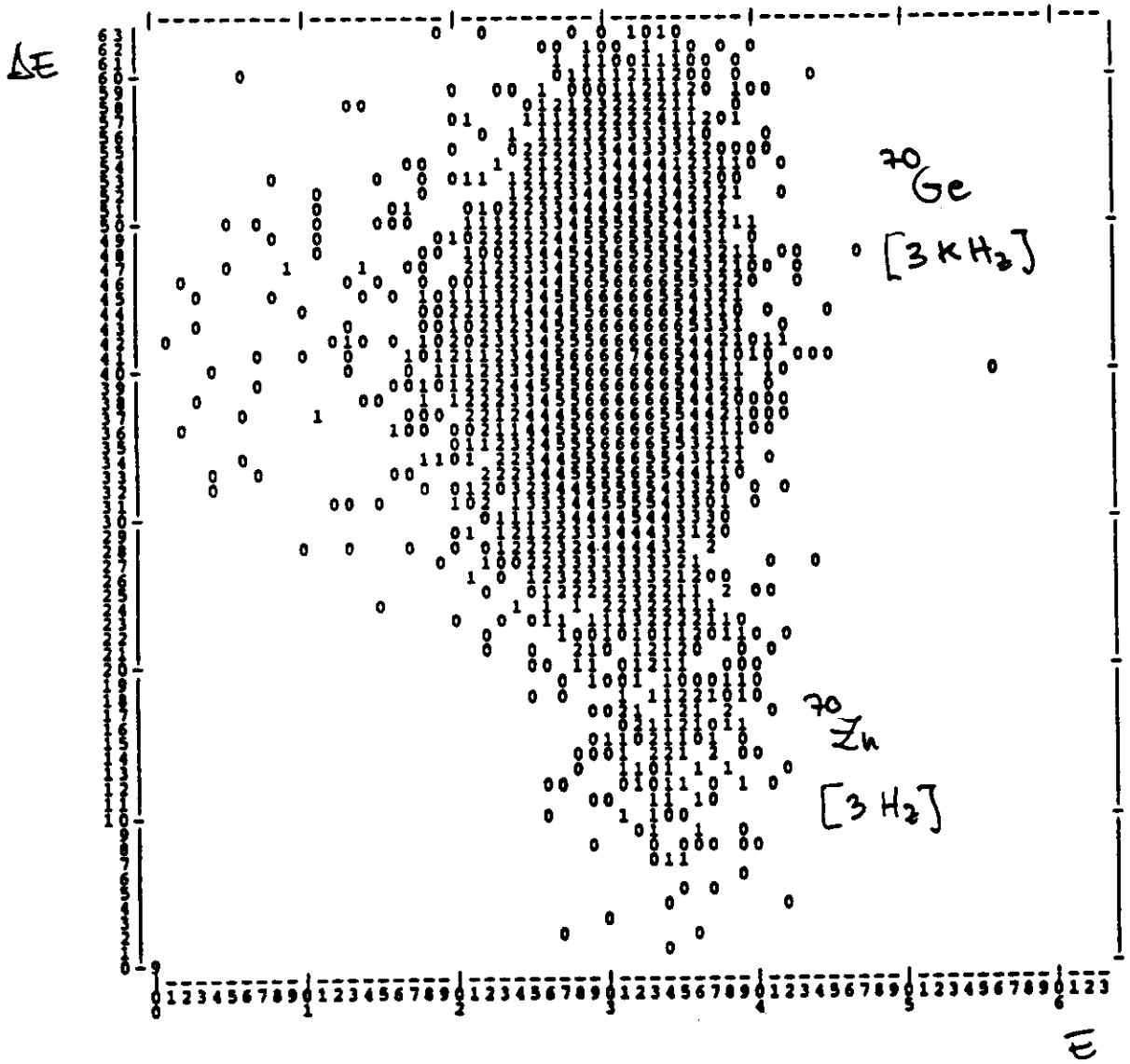

00SEC, TA 40MINUTES IN SOURCE, SOURCE SLITS CLOSED
RRAY:: TD2 GETA702ID2.27OCT87 012...9
-AXIS:: X CHANNELS 0 TO 63 OUT OF 64
-AXIS:: YY CHANNELS 0 TO 63 OUT OF 64
OGARITHMIC BASE = 2.00

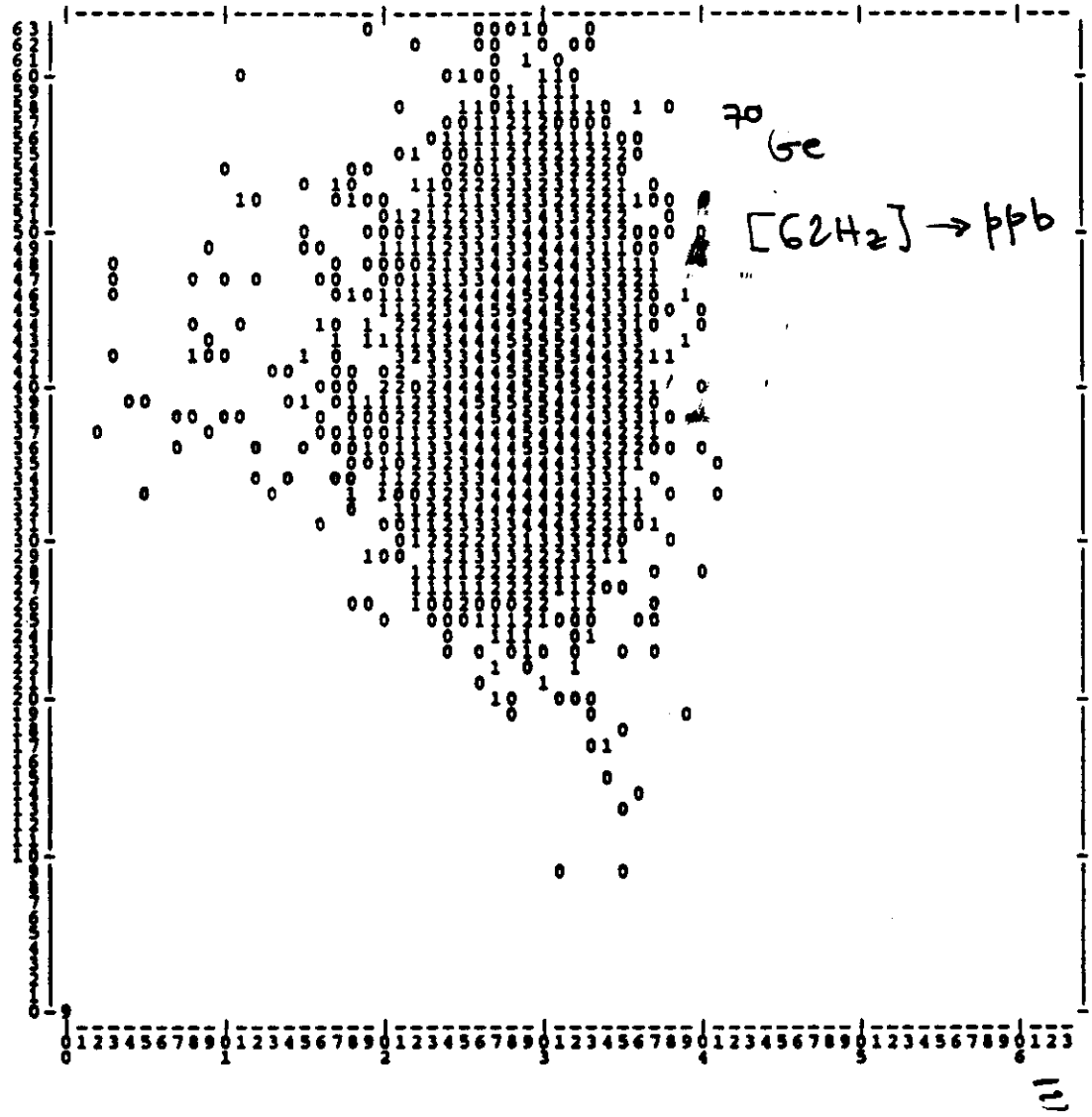

GAINA F., N.W. ...: 900 x10^- yr.

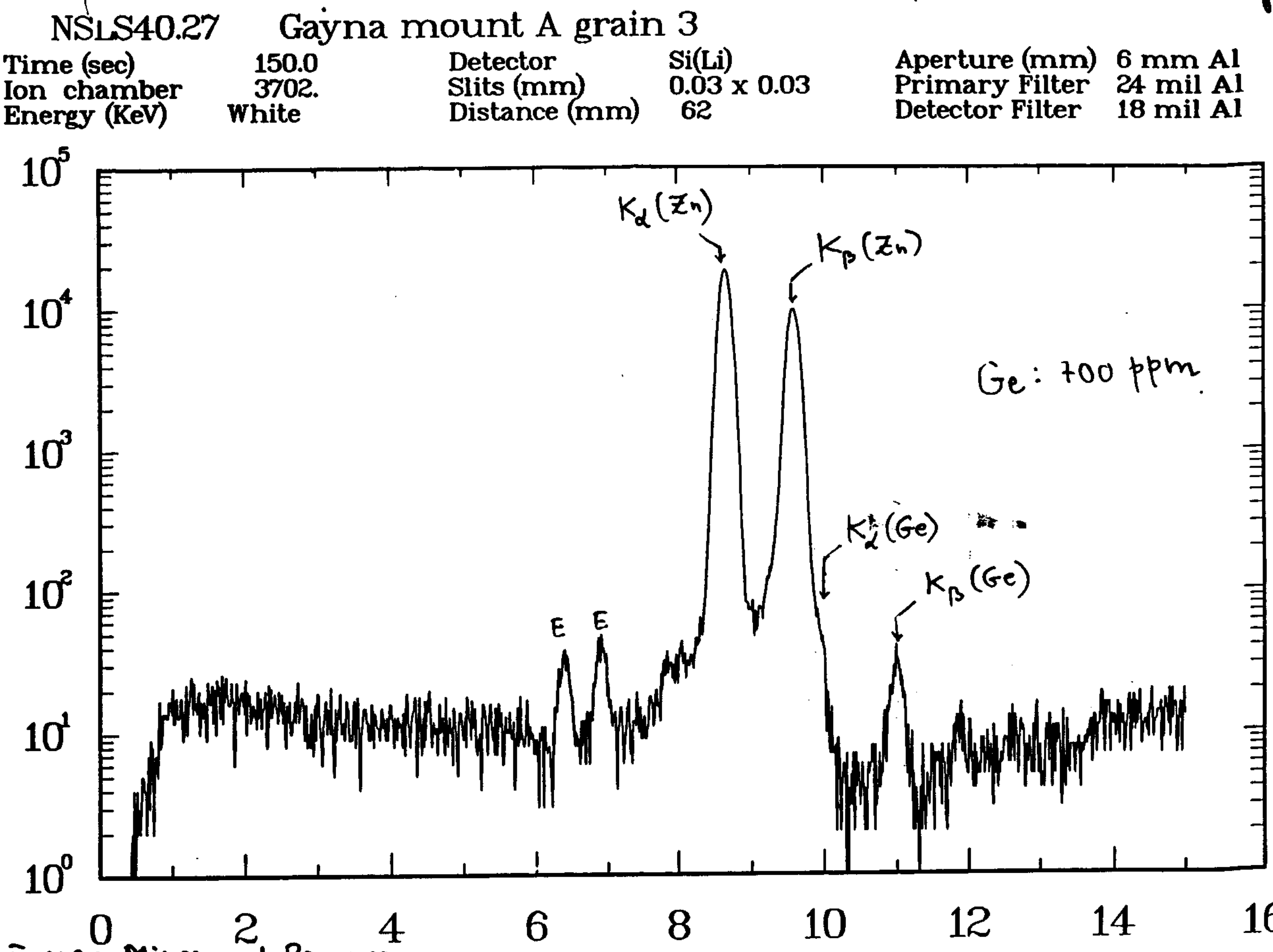

L. CABRI: Energy, Mines and Resources CANADA

M. RIVERS: Nat. Brookhaven Lab. USA

36

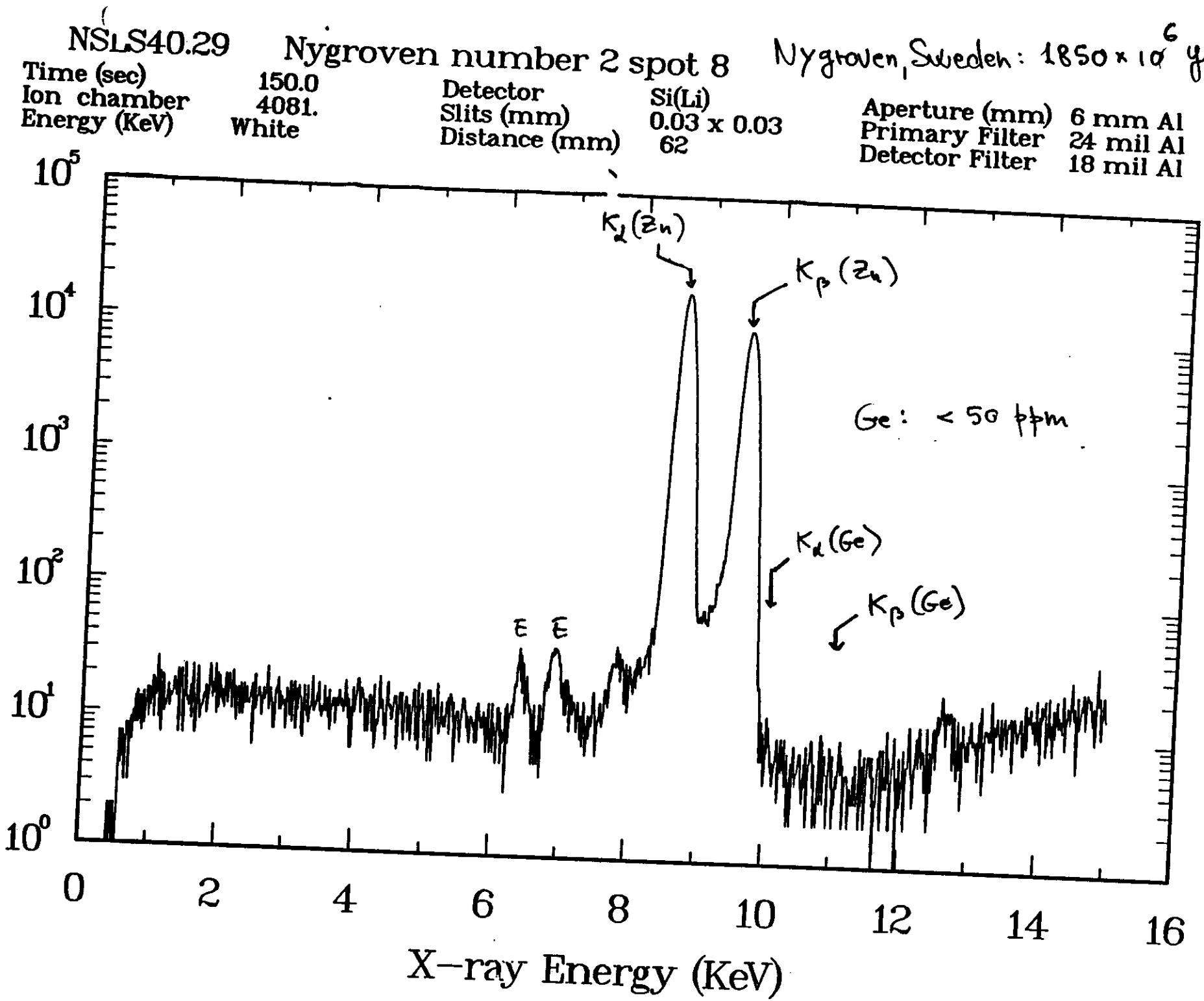
NSLS40.29 Nygroven number 2 spot 8 Nygroven, Sweden: 1850 x 10^6 yr.
Time (sec) 150.0
Ion chamber 4081.
Energy (KeV) White
Detector Si(Li)
Slits (mm) 0.03 x 0.03
Distance (mm) 62
Aperture (mm) 6 mm Al
Primary Filter 24 mil Al
Detector Filter 18 mil Al
10^5
10^4
10^3
10^2
10^1
10^0
$K_\alpha(Zn)$
$K_\beta(Zn)$
Ge: < 50 ppm
$K_\alpha(Ge)$
$K_\beta(Ge)$
E E
0 2 4 6 8 10 12 14 16
X-ray Energy (KeV)

PROTON DECAY

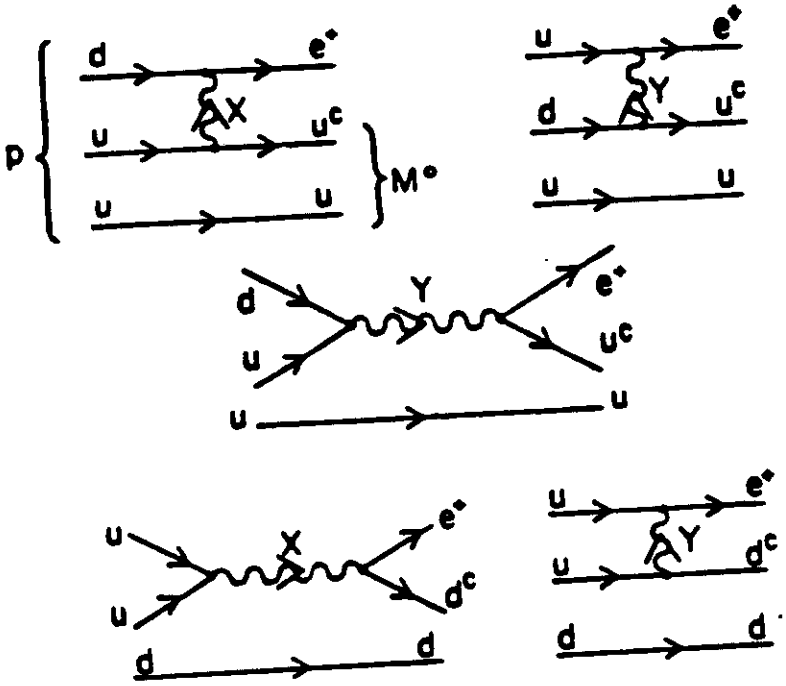

GUT : $\tau_p \sim 5 \times 10^{29\pm1}$ anni

$$^{130}_{52}Te \xrightarrow[\lambda_1]{\text{ε}} {}^{129}_{51}Sb \xrightarrow[9.6\,h]{\beta^-} {}^{129}Te \xrightarrow[67\,m]{\beta^-} {}^{129}I \xrightarrow[\lambda_2]{} {}^{129}Xe$$

→ $\tau_1 > 1.6 \times 10^{25}$ (^{129}Xe) EVANS & STEINBERG (77)

→ K.W. ALLEN: AMS (1981)

$\lambda_1 N_1 = \lambda_2 N_2$ $\quad \lambda_1 = 0.693 / \tau_1$

$\tau_1 = 10^{31}$ a

$\tau_2 = 1.6 \times 10^{7}$ a

^{130}Te : 34.5 %

^{129}I → ^{129}I

$N_2 \cong 1000$ atomi ^{129}I / Kg Te

10 ton → 10^7 at ^{129}I $\quad$ se I ~ 0.1 ppm

[cattiva ^{131}I (8 g)] $\quad ^{129}I / I \sim 10^{-14}$

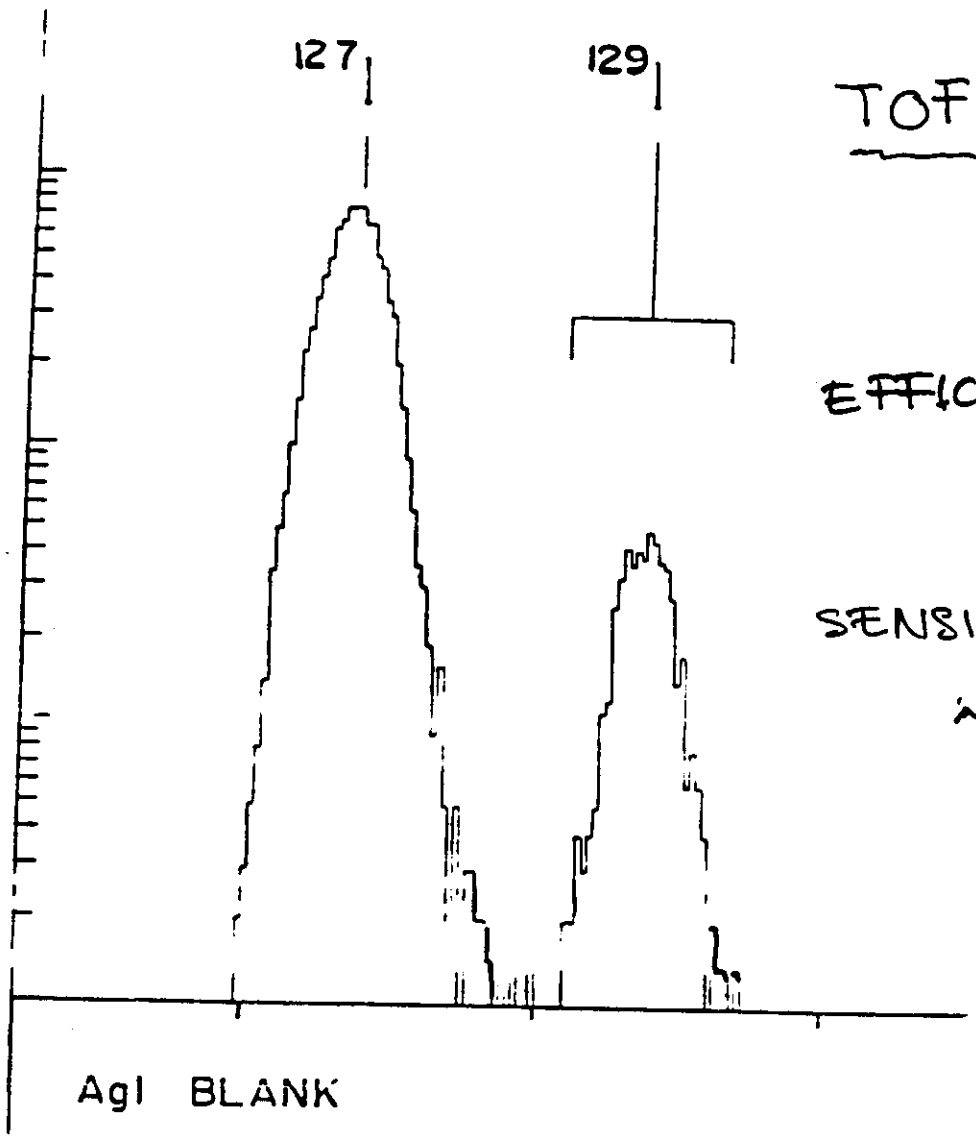

AgI BLANK

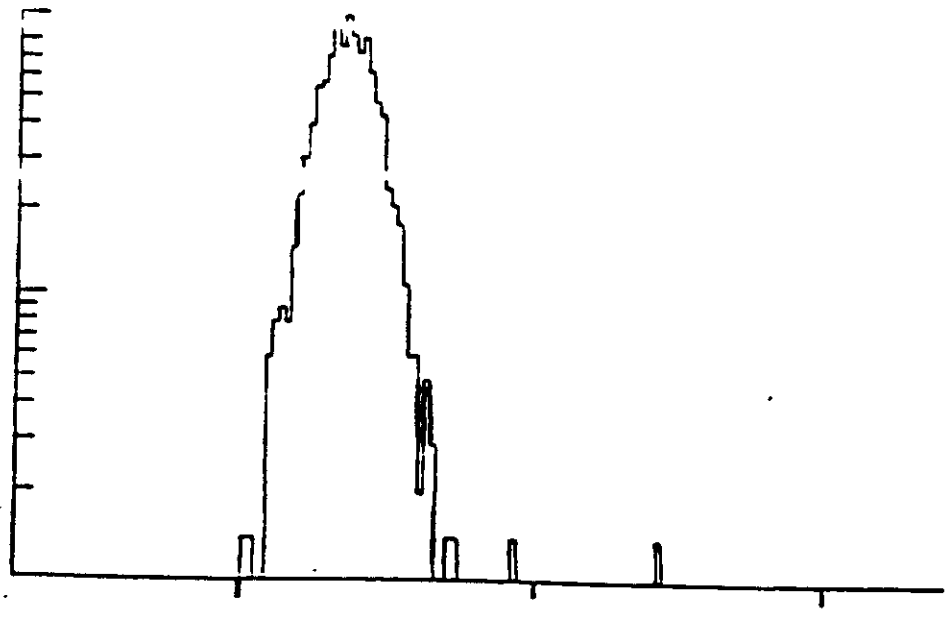

TIME of FLIGHT

TOF con MCP

EFFICENZA TOTALE:
$\sim 10^{-4}$

SENSIBILITÀ:
$\sim 10^{-14}$